ligases [Wel et al., 1995]. However, M249V mutant could be partially functional, because LIG4 knock-out mice show embryonic lethality [Frank et al., 2000]. LIG4 plays a critical role in both DNA replication and V(D)J recombination [Riballo et al., 1999; O'Driscoll et al., 2001]. Thus its deficit might cause the death of the cells with non-functional repair or recombination during meiosis or rearrangement of both T and B cell receptors, which promotes a progressive combined immunodeficiency in LIG4 syndrome. Such a slow progression of the disease as in our case might be one of the characteristic features of LIG4 syndrome.

We detected EBV-specific RNAs and latent proteins in the tumor cells in our case, although no EBV genome was detected in her peripheral blood by PCR. EBV infection to B cells causes infectious mononucleosis in immunocompetent individuals, but promotes lymphoproliferative disorders including malignant lymphoma in immunocompromised hosts particularly with profound T cell defect [Okano and Gross, 2000]. Thus, it is possible that her deficient immunosurveillance allowed the development of EBV-associated B cell lymphoma. Otherwise, the defects in damaged-DNA repair might be responsible for the development of her malignancy as seen in other chromosome breakage syndromes such as NBS and ataxia telangiectasia. There have been two cases with T cell leukemia, one case with B-cell lymphoma and one case with myelodysplasia complicated with LIG4 syndrome to date. Collectively, LIG4 syndrome patients are likely to be at increased risk for lymphoid malignancies.

The desquamative erythema, protracted diarrhea, and neutropenia during the reduced chemotherapy could be correlated with the defect in repair of DNA damage induced by the cytotoxic agents used for her treatment. Accordingly, haematopoietic stem cell transplantation that requires cytotoxic agents for myeloablation could be harmful for patients with this syndrome. Instead, anti-CD20 antibody (rituximab) or adoptive EBV-CTL therapy may be beneficial for EBV-associated lymphoma in such patients.

ACKNOWLEDGMENTS

We thank Dr. H. Kikuta for his analyzing EBV-DNA by PCR, and to Dr. Y. Sakiyama, Dr. F. Kuroki, Dr. M. Kaneda and Dr. M. Yoshida, and to staff at the Pediatric Ward, Hokkaido University Hospital for their substantial contribution. We also thank Dr. Ochs HD, University of Washington, for his helpful suggestion. This work was supported in part by Grant-in-Aid (No.14370237: IK, NK, KK and No. 14570714: MO) from the Ministry of Education, Science, Sports and Culture, Japan, and Grant 25060018-15 from the Ministry of Health, Labor and Welfare, Japan.

REFERENCES

Ben-Omram TI, Cerosaletti K, Concannon P, Weitzman S, Nezarati MM. 2005. A patient with mutations in DNA ligase IV: Clinical features and overlap with Nijmegen breakage syndrome. Am J Med Genet Part A 137A:283–287.

Buck D, Moshous D, de Chasseval R, Ma Y, le Deist F, Cavazzana-Calvo M, Fischer A, Casanova JL, Lieber MR, de Villartay JP. 2006. Severe combined immunodeficiency and microcephaly in siblings with hypomorphic mutations in DNA ligase IV. Eur J Immunol 36:224–235.

Enders A, Fisch P, Schwarz K, Duffner U, Pannicke U, Nikolopoulos E, Peters A, Orlowska-Volk M, Schindler D, Friedrich W, Selle B, Niemeyer C, Ehl S. 2006. A severe form of human combined immunodeficiency due to mutations in DNA ligase IV. J Immunol 176:5060–5068.

Frank KM, Sharpless NE, Gao Y, Sekiguchi JM, Ferguson DO, Zhu C, Manis JP, Horner J, DePinho RA, Alt FW. 2000. DNA ligase IV deficiency in mice leads to defective neurogenesis and embryonic lethality via p53 pathway. Mol Cell 5:993–1002.

Goode EL, Dunning AM, Kuschel B, Healey CS, Day NE, Ponder BA, Easton DF, Pharoah PP. 2002. Effect of germ-line genetic variation on breast cancer survival in a population-based study. Cancer Res 62:3052–3057.

Grawunder U, Zimmer D, Leiber MR. 1998. DNA ligase IV binds to XRCC4 via a motif located between rather than within its BRCT domains. Curr Biol 8:873–876.

O'Driscoll M, Cerosaletti KM, Girard PM, Dai Y, Stumm M, Kysela B, Hirsch B, Gennery A, Palmer SE, Seidel J, Gatti RA, Varon R, Oettinger MA, Neitzel H, Jeggo PA, Concannon P. 2001. DNA ligase IV mutation identified in patients exhibiting developmental delay and immunodeficiency. Mol Cell 8:1175–1185.

Okano M, Gross TG. 2000. A review of Epstein-Barr virus infection in patients with immunodeficiency disorders. Am J Med Sci 319:392–396.

Riballo E, Critchlow SE, Teo S-H, Doherty AJ, Priestley A, Broughton B, Kysela B, Beamish H, Plowman N, Arlett CF, Lehmann AR, Jackson SP, Jeggo PA. 1999. Identification of a defect in DNA ligase IV in a radio sensitive leukemia patient. Curr Biol 9:699–702.

Roddam PL, Rollinson S, O'Driscoll M, Jeggo PA, Jack A, Morgan GJ. 2002. Genetic variants of NHEJ DNA ligase IV can affect the risk of developing multiple myeloma, a tumor characterised by aberrant class switch recombination. J Med Genet 39:900–905.

van der Burg M, van Veelen LR, Verkaik NS, Wiegant WW, Hartwig NG, Barendregt BH, Brugmans L, Raams A, Jaspers NG, Zdzienicka MZ, van Dongen JJ, van Gent DC. 2006. A new type of radiosensitive T-B-NK+ severe combined immunodeficiency caused by a LIG4 mutation. J Clin Invest 116:137–145.

Weiss LM, Jaffe ES, Liu XF, Chen YY, Shibata D, Medeiros LJ. 1992. Detection and localization of Epstein-Barr viral genomes in angioimmunoblastic lymphadenopathy and angioimmunoblastic lymphadenopathy-like lymphoma. Blood 79:1789–1795.

Wel YF, Robins P, Carter K, Caldecott K, Pappin DJC, Yu GL, Wang RP, Shell BK, Nash RA, Schär P, Barnes DE, Haseltine WA, Lindahl T. 1995. Molecular cloning and expression of human cDNA encoding a novel DNA ligase IV and DNA ligase III, as enzyme active in DNA repair and recombination. Mol Cell Biol 15:3206–3216.

Yamada M, Matsuura S, Tsukahara M, Ebe K, Ohtsu M, Furuta H, Kobayashi I, Kawamura N, Okano M, Shouji R, Kobayashi K. 2001. Combined immunodeficiency, chromosomal instability, and postnatal growth deficiency in a Japanese girl: A new syndrome? Am J Med Genet 100: 9–12.

Hematopoietic stem cell–engrafted NOD/SCID/IL2Rγ^{null} mice develop human lymphoid systems and induce long-lasting HIV-1 infection with specific humoral immune responses

Satoru Watanabe,[1] Kazuo Terashima,[2] Shinrai Ohta,[3] Shigeo Horibata,[3] Misako Yajima,[4] Yoko Shiozawa,[1] M. Zahidunnabi Dewan,[2,3] Zhong Yu,[2] Mamoru Ito,[5] Tomohiro Morio,[6] Norio Shimizu,[1] Mitsuo Honda,[3] and Naoki Yamamoto[2,3].

[1]Department of Virology, Division of Medical Science, Medical Research Institute, Tokyo Medical and Dental University, Japan; [2]Department of Molecular Virology, Graduate School of Medicine, Tokyo Medical and Dental University, Japan; [3]AIDS Research Center, National Institute of Infectious Diseases, Tokyo, Japan; [4]Department of Infectious Diseases, National Research Institute for Child Health and Development, Tokyo, Japan; [5]Central Institute for Experimental Animals, Kanagawa, Japan; and [6]Department of Pediatrics and Developmental Biology, Graduate School of Medicine, Tokyo Medical and Dental University, Japan

Critical to the development of an effective HIV/AIDS model is the production of an animal model that reproduces long-lasting active replication of HIV-1 followed by elicitation of virus-specific immune responses. In this study, we constructed humanized nonobese diabetic/severe combined immunodeficiency (NOD/SCID)/interleukin-2 receptor γ-chain knockout (IL2Rγ^{null}) (hNOG) mice by transplanting human cord blood–derived hematopoietic stem cells that eventually developed into human B cells, T cells, and other monocytes/macrophages and dendritic cells associated with the generation of lymphoid follicle–like structures in lymphoid tissues. Expressions of CXCR4 and CCR5 antigens were recognized on CD4$^+$ cells in peripheral blood, the spleen, and bone marrow, while CCR5 was not detected on thymic CD4$^+$ T cells. The hNOG mice showed marked, long-lasting viremia after infection with both CCR5- and CXCR4-tropic HIV-1 isolates for more than the 40 days examined, with R5 virus–infected animals showing high levels of HIV-DNA copies in the spleen and bone marrow, and X4 virus–infected animals showing high levels of HIV-DNA copies in the thymus and spleen. Furthermore, we detected both anti–HIV-1 Env gp120– and Gag p24–specific antibodies in animals showing a high rate of viral infection. Thus, the hNOG mice mirror human systemic HIV infection by developing specific antibodies, suggesting that they may have potential as an HIV/AIDS animal model for the study of HIV pathogenesis and immune responses. (Blood. 2007; 109:212-218)

Introduction

Current animal models for either human immunodeficiency virus type 1 (HIV-1) or simian immunodeficiency virus (SIV) suffer from the lack of a system precisely mirroring human HIV infection and the progression to disease state.[1] In current animal models with HIV infection, such as chimpanzees, animals do not develop AIDS.[1] Past animal models for HIV infection have relied on humanized severe combined immunodeficiency (hSCID) mice models to study prospective anti-HIV drugs and vaccines. SCID-hu (Thy/Liv) mice, engrafted with human fetal thymus and liver tissue in the renal subcapsular region, were first reported as the small-animal model.[2] Because human T cells are generated within the engrafted thymus, this model has been used for the study of thymopoiesis[3-6] and hematopoiesis[7,8] under the burden of HIV-1 infection. However, this model allows for a limited systemic HIV-1 infection, which is restricted mainly to the engrafted thymus. Another HIV mouse model, hu-PBL–SCID mice engrafted with human peripheral blood mononuclear cells (PBMCs),[9] has been actively used as a tool in developing antiretroviral therapy.[9-11] However, the infection persists for only a short time in association with rapid loss of CD4$^+$ T cells because there is no active hematopoiesis or thymopoiesis.[9,12,13] Furthermore, these mouse models fail to mirror certain key aspects of the human immune response, lacking normal lymphoid tissue and functional human antigen-presenting cells such as dendritic cells (DCs).[14] Thus, although these mouse models are valuable as animal models for HIV infection, the development of a mouse model more analogous to human HIV infection is needed if we are to better understand HIV pathogenesis and develop successful anti-HIV therapies and preventive vaccines.

To solve the difficult issue about the development of an ideal HIV mouse model, we initially selected a humanized nonobese diabetic (NOD)/SCID interleukin-2 receptor (IL-2R) γ-chain knockout (NOG) mouse[15] as a model animal because it has been suggested that multilineage cells, including human T, B, and natural killer (NK) cells, differentiate in these mice when given transplants of human CD34$^+$ hematopoietic stem cells.[16-18] In the current study, we further reveal the kinetics of differentiation of human B and T cells, monocytes/macrophages, and DCs in the mice that received transplants, and we characterize the animals by infection with both CCR5 (R5)– and CXCR4 (X4)-tropic HIV strains. Since our hNOG mice show stable and systemic infection of both R5- and X4-tropic HIV for more than

Submitted April 20, 2006; accepted August 12, 2006. Prepublished online as *Blood* First Edition Paper, September 5, 2006; DOI 10.1182/blood-2006-04-017681.

The publication costs of this article were defrayed in part by page charge payment. Therefore, and solely to indicate this fact, this article is hereby marked "advertisement" in accordance with 18 USC section 1734.

the 40 days studied, and HIV-specific antibodies are detectable in the animals with high plasma viral loads and HIV-DNA copy numbers, we also discuss the suitability of HIV-hNOG mice as an animal model for HIV-1 infection.

Materials and methods

Transplantation of human CB-derived hematopoietic stem cells in NOG mice

Human cord blood (CB) was obtained from Saiseikai Central hospital (Minato-ku, Tokyo, Japan) and Tokyo Cord Blood Bank (Katsushika-ku, Tokyo, Japan) after obtaining informed consent. All research on human subjects was approved by the Institutional Review Board of each institution participating in the project. CB mononuclear cells were separated by Ficoll-Hypaque density gradient. $CD34^+$ hematopoietic stem cells were isolated using a magnetic-activated cell sorting (MACS) Direct CD34 Progenitor Cell Isolation Kit (Miltenyi Biotec, Bergisch Gladbach, Germany) according to the manufacturer's instructions. More than 95% of $CD34^+$ cells were positively selected after 2 time-enrichment manipulations. Cells were either immediately used for the transplantation or frozen until use. NOG mice were obtained from the Central Institute for Experimental Animals (Kawasaki, Japan) and maintained under specific pathogen-free (SPF) conditions in the animal facility of the National Institute of Infectious Diseases (NIID; Tokyo, Japan). Mice used in these studies were free of known pathogenic viruses, herpes viruses, bacteria, and parasites. They were housed in accordance with the Guidelines for Animal Experimentation of the Japanese Association for Laboratory Animal Science (1987) under the Japanese Law Concerning the Protection and Management of Animals, and were maintained in accordance with the guidelines set forth by the Institutional Animal Care and Use Committee of NIID, Japan. Once approved by the Institutional Committee for Biosafety Level 3 experiments, these studies were conducted at the Animal Center, NIID, Japan, in accordance with the requirements specifically stated in the laboratory biosafety manual of the World Health Organization. Female mice (6 to 10 weeks old) were irradiated (300 cGy) and 1×10^4 to 1.2×10^5 $CD34^+$ cells were intravenously injected within 12 hours.

Flow cytometry

The purity of CB-derived $CD34^+$ cells after separation was evaluated by double staining with FITC-conjugated anti–human CD45 (J.33) and PE-conjugated anti–human CD34 (Class III 581) (all from Beckman Coulter, Fullerton, CA). After transplantation (1-7 months), peripheral blood, spleens, bone marrow (BM), and thymi were collected for flow cytometric analysis following staining with the following monoclonal antibodies (mAbs): FITC-conjugated anti–human CD45 (J.33), CD3 (UCHT1), CD4 (13B8.2), CD19 (J4.119), CD45RO (UCHL1) (all from Beckman Coulter), and CCR5 (2D7; BD Pharmingen, San Diego, CA); PE-conjugated anti–human CD4 (13B8.2), CD8 (B9.11), CD19 (J4.119), CD45RA (ALB11) (all from Beckman Coulter), and CXCR4 (44717; R&D Systems, Minneapolis, MN); anti–mouse CD45 (YW62.3; Beckman Coulter); ECD-conjugated anti–human CD45 (J.33; Beckman Coulter); and PC5-conjugated anti–human CD8 (T8) and CD14 (Rm052) (all from Beckman Coulter). Flow cytometric analysis was conducted by 2- or 4-color staining using an EpicsXL (Beckman Coulter).

Immunohistochemistry

Organs were snap-frozen following embedding in OCT compound (Sakura Finetechnical, Tokyo, Japan). Frozen sections were air-dried and fixed in acetone. HIV-1–infected organs were fixed in 4% paraformaldehyde and embedded in OCT compound following immersion in gradient sucrose (5%-30%). Fixed samples were stained with the following mAbs: anti–human CD45 (1.22/4014; Nichirei, Tokyo, Japan), CD3 (UCHT1; DAKO, Glostrup, Denmark), CD20 (L26; DAKO), CD68 (KP1; DAKO), CD205 (MG38; eBioscience, San Diego, CA), and DRC-1 (R4/23; DAKO) for follicular dendritic cells (FDCs); anti–mouse FDC-M1 (BD Pharmingen) for murine FDCs; and HIV-1 Gag p24 (DAKO) for detection of infected cells. Biotin-labeled goat $F(ab')_2$ anti–mouse immunoglobulin (Ig; ICN Biomedicals, Aurora, OH)– or biotin-labeled mouse $F(ab')_2$ anti–rat IgG (Jackson ImmunoResearch Laboratories, West Grove, PA) was used as the secondary antibody. Samples were treated with alkaline phosphatase (AP) or horseradish peroxidase (HRP)–streptavidin conjugate (ZYMED Laboratories Inc, San Francisco, CA). BCIP/NBT, DAB, or AEC (all from DAKO) was used for the visualization. Photographs were taken by light microscopy (Leica DMRA; Leica Microsystems Wetzlar, Wetzlar, Germany) using Leica HC PLAN APO lenses (10×/0.40 NA PH1). Leica Q550 was used for image processing.

Measurement of human Igs in mice plasma

Plasma concentrations of human IgM, IgG, and IgA in NOG mice that received transplants of human stem cells were determined by conventional human Ig quantitation assay at BML Inc (Tokyo, Japan).

Cells and viruses

Human embryonic kidney 293T cells and monkey kidney COS7 cells were cultured in RPMI 1640 supplemented with 10% fetal bovine serum (FBS) and antibiotics. The 293T cells and COS7 cells were used for transfection of DNA plasmids containing HIV-1_{JRCSF} and simian/human immunodeficiency virus (SHIV)–C2/1, respectively. The SHIV-C2/1 strain contains the *env* gene of pathogenic HIV-1 strain 89.6.[19] Cell-free supernatant was collected and stored at −80°C before use. A primary clinical isolate, HIV-1_{MNp}, was kindly provided by Dr J. Sullivan of the University of Massachusetts Medical School (Worcester, MA). PBMCs isolated from HIV-1–seronegative individuals were cultured in RPMI 1640 supplemented with 10% FBS and antibiotics with 5 μg of phytohemagglutinin (PHA)/mL for 3 or 7 days (PHA-PBMCs). HIV-1_{MNp} was propagated in PHA-PBMCs, and cell-free virus stocks were stored at −80°C.

The 50% tissue-culture infectious dose ($TCID_{50}$) was determined using PHA-PBMCs and the endpoint dilution method. A 4-fold series of dilution was prepared from the virus stock, and then cells were mixed and cultured for 7 days for X4–HIV-1 and 14 days for R5–HIV-1 in RPMI 1640 supplemented with 20% FBS and antibiotics. The endpoints were determined by screening for the p24 antigen using Lumipulse (Fujirevio, Tokyo, Japan).

HIV-1 infection

All procedures for the infection and maintenance of NOG mice were performed in Biosafety Level 3 facilities at NIID under standard caging conditions. On days 102 to 132 after stem cell transplantation, 16 mice were inoculated intravenously with R5-tropic HIV-1_{JRCSF} (65 000 $TCID_{50}$) or X4-tropic SHIV-C2/1 (50 000 $TCID_{50}$). On days 18 to 43 after inoculation, plasma was collected to determine HIV-RNA copy numbers, and spleen cells were prepared as single-cell suspensions to analyze the CD4/CD8 ratio using flow cytometry. A number (14) of other mice were inoculated intravenously with R5-tropic HIV-1_{JRCSF} (200 or 65 000 $TCID_{50}$) or X4-tropic HIV-1_{MNp} (180 or 20 000 $TCID_{50}$) on days 126 to 146 after transplantation. On days 18 to 40 after inoculation, plasma was collected for the determination of HIV-RNA copy numbers, and single-cell suspensions of the spleen, BM, and thymus were prepared for HIV-DNA measurement. The CD4/CD8 ratio in the spleen and percentages of human $CD45^+$ cells in organs were analyzed using flow cytometry.

Virologic analysis

Plasma viral RNA copy numbers were measured using a real-time quantification assay based on the TaqMan system (Applied Biosystems, Foster City, CA). Plasma viral RNA was extracted and purified using a QIAamp Viral RNA Mini Kit (Qiagen, Valencia, CA). The RNA was subjected to reverse transcription (RT) and amplification using a TaqMan One-Step RT–polymerase chain reaction (PCR) Master Mix Reagents Kit (PE Biosystems, Foster City, CA) with HIV-1 gag consensus primers

(forward, 5′-GGACATCAAGCAGCCATGCAA-3′; and reverse, 5′-TGCTATGTCACTTCCCCTTGG-3′) and an HIV-1 gag consensus TaqMan probe (FAM-5′-ACCATCAATGAGGAAGCTGCAGAA-3′-TAMRA). For SHIV-C2/1 analysis, primers (forward, 5′-AATGCAGAGCCCCAAGAAGAC-3′; and reverse, 5′-GGACCAAGGCCTAAAAAACCC-3′) and a TaqMan probe (FAM-5′-ACCATGTTATGGCCAAATGCCCAGAC-3′-TAMRA) were designed for targeting the SIVmac239 gag region.[20] Probed products were quantitatively monitored by their fluorescence intensity with the ABI7300 Real-Time PCR system (PE Biosystems). To obtain control RNA for quantification, HIV-1 gag RNA and SIVmac239 gag RNA were synthesized using T7 RNA polymerase and pKS460. Viral DNA was extracted and purified using a QIAamp DNA Mini Kit (Qiagen). Determination of HIV-1 DNA copy numbers was performed by real-time PCR assay with TaqMan Master mixture (PE Biosystems). Primers (forward, 5′-GGCTAACTAGGGAACCCACTG-3′; and reverse, 5′-CTGCTAGAGATTTTCCACACT-3′) and probes (FAM-5′-TAGTGTGTGCCCGTCTGTTGTGTGAC-3′-TAMRA) were designed for targeting the HIV-1 long terminal repeat region, R/U5. The viral DNA was quantified using LightCycler (Roche Diagnostics, Almere, The Netherlands). Viral RNA and DNA were calculated based on the standard curve of control RNA and DNA. All assays were carried out in duplicate.

HIV-antigen ELISA

Levels of anti–HIV-1 Igs against recombinant HIV-1_{IIIB} Env gp120, recombinant HIV-1_{MN} Env gp120, and recombinant HIV-1_{IIIB} Gag p24 (all from ImmunoDiagnostics Inc, Woburn, MA) in plasma from HIV-1–infected and –uninfected control mice were determined using a standard enzyme-linked immunosorbent assay (ELISA). Microplates (96-well) were coated overnight with 200 ng/well antigens, and plasma diluted 1:20, 1:60, and 1:180 with PBS were incubated for 1 hour. AP-labeled anti–human Igs (γ, α, and μ; Sigma-Aldrich, St Louis, MO) were used as secondary antibodies. P-nitrophenylphosphate (pNPP) Solution (WAKO Chemical USA, Richmond, VA) was used for the visualization. The enzyme reaction was stopped by addition of 0.1 M NaOH and read at 405 nm. All assays were carried out in triplicate.

Statistical analysis

Data were expressed as the mean value ± standard deviation (SD). Significant differences between data groups were determined by 2-sample Student *t* test analysis. A *P* value less than .05 was considered significant.

Results

Reconstitution of human lymphoid systems in hNOG mice

The initial studies describing the construction of humanized SCID mice used the human PBMC for infection of immunodeficiency viruses.[9,12,21] However, these hu-PBL-SCID mice showed a partial infection to the R5 virus and a relatively limited period of viral replication. To construct a more suitable mouse model mimicking HIV-1 infection in humans, we selected human CB stem cells as a transplant for NOG mice. NOG mice were inoculated intravenously with human CD34$^+$ hematopoietic stem cells, and their development of human lymphoid systems were then monitored. After transplantation (2 months), human CD45$^+$ leukocytes were recognized in both PB and the spleen, but most of the cells were human B cells (Figure 1A). Human T cells began to be recognized clearly in PB and the spleen 4 months after transplantation (Figure 1B) and gradually increased in level, as did human B cells (Figure 1C).

In Figure 1D, we summarized percentages of human CD3$^+$ T cells in human CD45$^+$ cells from 38 mice from 39 to 213 days after transplantation. Human CD3$^+$ T cells clearly increased 100 days after transplantation in both PB and the spleen. After transplantation (4 months), human CD3$^+$ T cells in the spleen preferably expressed CD45RA rather than CD45RO (70.8% ± 13.4% and 27.3% ± 38.8% in CD3$^+$ T cells, respectively; n = 5; Figure 1E), demonstrating that most of the T cells were in a naive state. In addition, plasma taken from 5 mice 113 to 143 days after transplantation showed that all mice produced human IgM, with concentrations ranging from 0.025 to 0.5 g/L, and that human IgG and IgA was also detected in some of the mice (ranges, 0.015-0.18 g/L and 0.003-0.012 g/L, respectively) (data not shown).

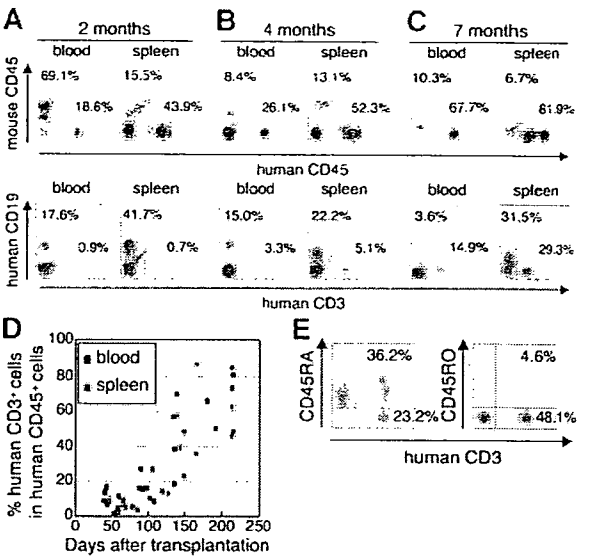

Figure 1. Flow cytometric analysis of human T cells in the peripheral blood and spleen in NOG mice given intravenous transplants of human CB-derived CD34$^+$ cells. (A-C) Representative profiles of the mice 2 months (A), 4 months (B), and 7 months (C) after transplantation. The ratio of human to murine CD45$^+$ cells and that of human CD3$^+$ to CD19$^+$ cells show an incremental increase in human CD45$^+$ cells and human CD3$^+$ cells from 2 to 7 months. (D) Change of net percentages of human CD3$^+$ T cells among human CD45$^+$ cells in peripheral blood and the spleen from 38 mice 39 to 213 days after transplantation. (E) CD45RA is more efficiently expressed than CD45RO on human CD3$^+$ T cells in spleen. A gate was set on the human CD45$^+$ population. The fluorescence-activated cell sorting (FACS) profile is representative of 1 in a group of 5 mice.

By 7 months after transplantation, human CD45$^+$ leukocytes comprised more than 80% to 90% of mononuclear cells in the spleen (Figure 1C), and most of the mice showed symptoms of a wasting condition and a hunched back. Based upon these results, we determined that the suitable period for HIV inoculation would be 4 to 5 months after transplantation.

Formation of lymphoid structures, including monocytes/macrophages, DCs, and FDCs

Next, using the hNOG mice at 4 months after transplantation, we investigated lymphoid structure formation and the development of human monocytes, macrophages, DCs, and FDCs, which are very important factors not only for elicitation of immune responses against foreign antigens, but also for the spread of HIV-1 infection in a body.[22-24] Human CD14$^+$ monocytes were detected in PB, the spleen, and BM using flow cytometry (Figure 2A). During immunohistochemical analysis, human CD45$^+$ leukocytes gathered in a form of follicle-like structures (FLSs) at the end of the central artery in the spleen (Figure 2B). From a serial section of the same region (Figure 2B-G), these structures consisted mainly of human CD20$^+$ B cells (Figure 2C) admixed with a small number of human CD3$^+$ T cells (Figure 2D). Hardly any human FDCs positive for DRC-1 were detected (data not shown), whereas a

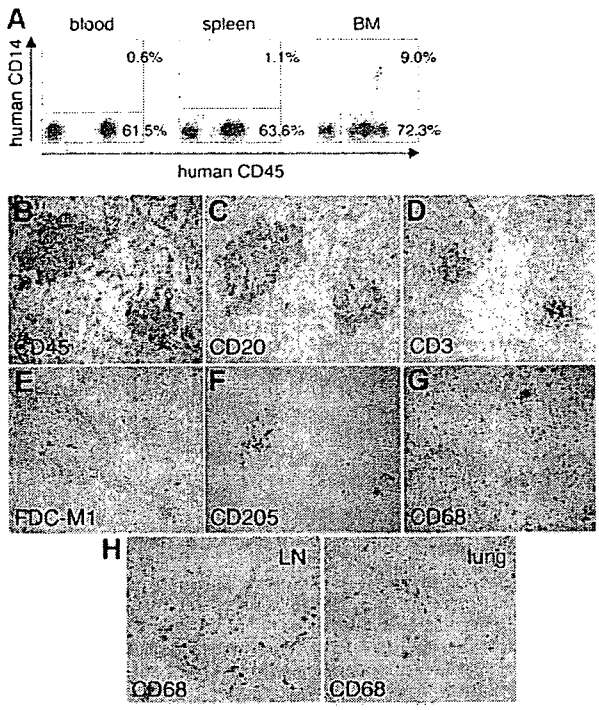

Figure 2. Flow cytometric analysis and immunohistochemical analysis of the expression of myelomonocytic markers in hNOG mice 4 months after transplantation. (A) Human CD14$^+$ monocytes/macrophages are recognized in peripheral blood, the spleen, and BM. (B-G) Immunohistochemical findings from serially sectioned spleen for the expressions of human CD45 (B), human CD20 (C), human CD3 (D), murine FDC (E), human CD205 (F), and human CD68 (G). (H) Human CD68$^+$ macrophages are also detected in the medulla of the LN and lung. Visualization was performed with BCIP (B-D, F-G), DAB (E), and AEC (H). Original magnification, ×100.

loose network of murine FDCs positive for FDC-M1 was recognized in the distal portion of the FLSs (Figure 2E). Human CD205$^+$ DCs were predominantly detected in a cluster form within the FLSs (Figure 2F), while human CD68$^+$ macrophages were scattered throughout the spleen (Figure 2G). Many human CD68$^+$ macrophages were also observed in various other organs, including the lymph nodes (LNs) and the lungs (Figure 2H).

Expression of HIV-1 coreceptors on CD4$^+$ cells in various tissues

Since the development of lymphoid tissues was recognized in hNOG mice, we focused on the expressions of HIV-1 coreceptors CXCR4 and CCR5 on human CD4$^+$ cells in these tissues. CXCR4 antigen was expressed in 36.5% ± 4.2% (n = 4) of the CD4$^+$ cells in PB (Figure 3A) and 78.1% ± 17.1% (n = 5) in the spleen (Figure 3B). CCR5$^+$ cells were detected in 15.5% ± 1.8% (n = 4) of CD4$^+$ cells in PB and 28.6% ± 12.6% (n = 5) in the spleen (Figure 3A-B). In the thymus, CD4$^+$CD8$^+$ thymocytes existed in 82.9% ± 4.4% (n = 5) as well as small numbers of CD4$^+$CD8$^-$ cells (6.4% ± 2.4%; n = 5) and CD4$^-$CD8$^+$ cells (7.7% ± 3.0%; n = 5), with the CXCR4 antigen expressed in 50.1% ± 4.5% (n = 5) of CD4$^+$ cells, while, as with normal human thymocytes,[25] CCR5$^+$ cells were almost undetectable, with less than 1% (0.6% ± 0.1%; n = 5) (Figure 3C). Human CD3$^+$ T cells and CD14$^+$ monocytes in BM were detected only in 3.2% ± 2.1% and 5.8% ± 3.8%, respectively, while CD4$^+$ cells were recognized in 18.1% ± 6.5%, with many expressing both CXCR4 (75.0% ± 23.1%) and CCR5 (81.3% ± 6.6%; n = 5; Figure 3D). Thus, distributions of HIV-1 coreceptor–positive cells in these lymphoid tissues suggest that the hNOG mice allow for sufficient development of human cells to make the study of HIV-1 pathogenesis possible.

Both R5- and X4-tropic HIVs efficiently infect and replicate in hNOG mice

In our preliminary study, using low and high doses of challenge virus, no viral infection was detected in any of the virus-inoculated hNOG mice at 7 days after infection, while some showed detectable plasma viral loads at 14 days (data not shown). Then, we prepared 16 hNOG mice that received transplants of stem cells and inoculated them with a high dose of R5-tropic HIV-1$_{JRCSF}$ (65 000 $TCID_{50}$) and X4-tropic SHIV-C2/1 (50 000 $TCID_{50}$) intravenously through the tail vein at 102 to 132 days after transplantation. Upon HIV-1$_{JRCSF}$ infection, viral copy numbers in plasma rose to a level of 1.6×10^5 to 5.8×10^5 copies/mL (n = 4) on day 33 and 2.0×10^5 to 4.7×10^5 copies/mL on day 43 (n = 4) (Figure 4A). Moreover, for SHIV-C2/1 infection, viral copy numbers in plasma were 1.6×10^3 to 3.2×10^5 copies/mL on day 18 (n = 4) and reached 5.4×10^4 to 1.1×10^5 copies/mL on day 42 (n = 4; Figure 4B). In these mice, no significant decline in the CD4/CD8 ratio was observed throughout entire period of follow-up for the R5-tropic virus infection, while CD4$^+$ cell decline was detected for the X4-tropic virus infection on day 42 after infection (P = .044) but not on day 18 after infection (Figure 4C). Four mice that did not receive transplants of human stem cells showed no detectable levels of plasma viral load (less than 500 copies/mL) following HIV/SHIV inoculation (data not shown).

To confirm HIV infection, we used immunohistochemistry to detect the presence of the p24 antigen of the HIV-1 Gag protein in various tissues of mice showing viremia. p24$^+$ cells were clearly identified in the spleen, LN, and lungs (Figure 4D), which include macrophage-like cells.

Different distributions of R5- and X4-tropic viruses in lymphoid tissues

A number of mice (14) were further analyzed for HIV-1 infection on days 126 to 146 after transplantation with a low dose (200 $TCID_{50}$) or a high dose (65 000 $TCID_{50}$) of R5-tropic HIV-1$_{JRCSF}$ and a low dose (180 $TCID_{50}$) or a high dose (20 000 $TCID_{50}$) of X4-tropic HIV-1$_{MNp}$. Consequently, 2 of the 4 mice given a low

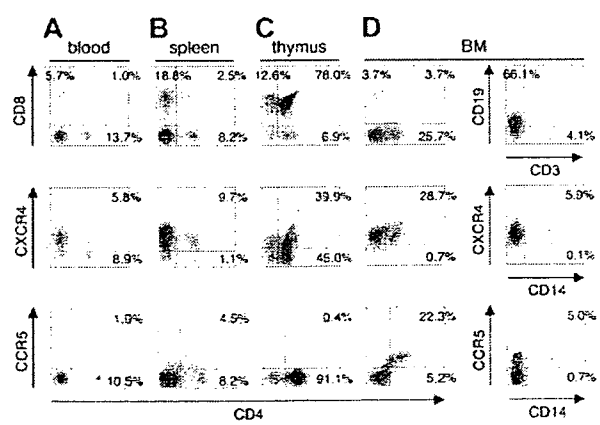

Figure 3. Surface expression of HIV-1 coreceptors on CD4$^+$ cells in various organs of mice 4 months after transplantation. A representative FACS profile of human CXCR4 and CCR5 on CD4$^+$ cells shows the existence of CXCR4$^+$CD4$^+$ and CCR5$^+$CD4$^+$ cells in blood (A), spleen (B), and BM (D), but no CCR5$^+$CD4$^+$ cells in the thymus (C). BM results show that many CD4$^+$ cells are neither CD3$^+$ T cells nor CD14$^+$ monocytes. A gate was set on the human CD45$^+$ population.

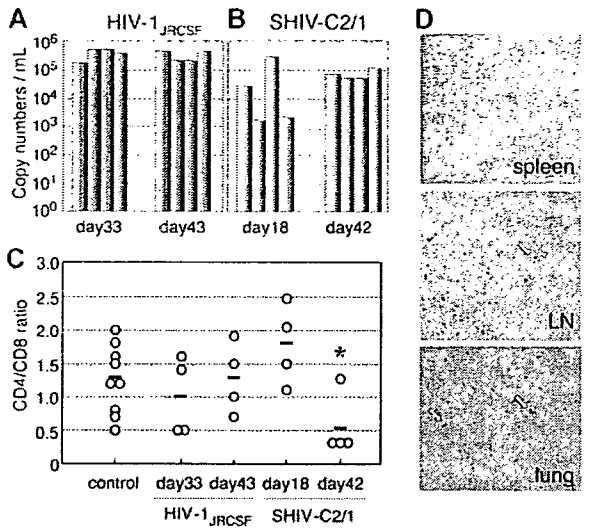

Figure 4. The numbers of RNA viral copies in plasma, CD4+/CD8+ T-cell ratios in the spleen, and p24 detection in the immunohistochemistry of HIV/SHIV-infected mice. (A) Viral copy numbers of 8 mice inoculated with a high infectious dose of HIV-1_{JRCSF} (65 000 $TCID_{50}$) and killed on days 33 and 43 after inoculation. (B) Viral copy numbers of 8 mice inoculated with a high infectious dose of SHIV-C2/1 (50 000 $TCID_{50}$) and killed on days 18 and 42 after inoculation. Note that all the mice showed high levels of viremia that lasted more than 40 days after inoculation. (C) CD4/CD8 cell ratios in the spleens of 16 infected mice and 9 uninfected control mice. Control mice were not inoculated with HIV/SHIV and were killed on days 105 to 166 after stem cell transplantation. There was no significant rapid loss of CD4+ cells in HIV-1_{JRCSF}–infected mice, while a decline of the CD4/CD8 ratio was detected in SHIV-C2/1–infected mice on day 42 after infection compared with uninfected control mice (*$P < .05$). The short bars indicate the means of each group. (D) P24+ cells are clearly observed in the spleen, LNs, and lungs. Arrow indicates p24 positive for macrophage-like cells. Original magnification, ×100.

dose of HIV-1_{JRCSF} and 2 of the 3 mice given a low dose of HIV-1_{MNp} were successfully infected (Table 1), suggesting that each dose represents an approximately 50% infectious dose of HIV for hNOG mice. High HIV-DNA copy numbers were mainly detected in the spleen and BM of the HIV-1_{JRCSF} –infected mice, and in the thymus and spleen of the HIV-1_{MNp}–infected mice, while their BM showed lower copy numbers (Table 1).

Generation of HIV-specific antibodies in hNOG mice at a high multiplicity of infection

We then tested for generation of human antibodies against HIV-1 from these 14 mice by HIV antigen-specific ELISA. The sera of mice no. 136-3 and no. 157-3 infected with HIV-1_{JRCSF} and HIV-1_{MNp}, respectively, showed significant levels of human antibodies specific for HIV-1_{IIIB}-Env gp120 (Figure 5A), HIV-1_{MN}-Env gp120 (Figure 5B), and HIV-1_{IIIB}-Gag p24 (Figure 5C). In addition, no. 157-4 sera from an HIV-1_{MNp}–infected animal was also weakly positive for their Env and Gag antigens. These animals showed intense plasma viral loads and enhanced proviral DNA copies in the spleen, BM, and thymus (Table 1), suggesting that hNOG mice inoculated with high doses of HIV and showing high rates of viral infection develop HIV-1–specific humoral immune responses that are analogous to those seen in human anti-HIV B-cell responses.

Discussion

Current small-animal models fall short of accurately mirroring human HIV-1 infection and thus have limited usefulness in analyzing the natural course of its progression to the disease state and in developing antiviral countermeasures. Although successful HIV-1 infections in immunodeficiency mice humanized with PBMCs have been reported,[12,13,21] transplanted human cells are soon depleted and do not elicit virus-specific immune responses, shedding little light on pathogenesis and vaccine development. By using NOG mice that received hematopoietic stem cell transplants showing high rates of viral infection, we demonstrated HIV-specific antibody responses and viral infection parameters, including the following: (1) similar levels of susceptibility to both R5- and X4-tropic HIV-1; (2) high levels of viremia stably observed over 40 days; (3) immunohistochemical detection of infected cells in various organs; and (4) a distinct tissue distribution for R5- versus X4-tropic HIV-1s.

Among CD4+ T cells, CXCR4 antigen is primarily expressed on naive and CCR5 on activated or memory cells.[26] hu-PBL-SCID mice become susceptible to R5-tropic HIV-1 strains,[27] since T cells

Table 1. Comparison of viral RNA copies in plasma and HIV-DNA copies in the spleen, BM, and thymus from hNOG mice receiving low- and high-dose viral inoculations

Mouse ID no.	HIV strain	$TCID_{50}$	Time after inoculation, d	RNA viral copies/mL	CD4/CD8 ratio	HIV-DNA copies/10^6 human cells		
						Spleen	BM	Thymus
Low-dose viral inoculation group								
113-1	HIV-1_{JRCSF}	200	18	6 240	1.8	34 177	11 785	3 495
112-2	HIV-1_{JRCSF}	200	18	<500	1.2	< 100	< 100	< 100
113-2	HIV-1_{JRCSF}	200	40	6 177	1.6	25 855	27 920	3 473
112-3	HIV-1_{JRCSF}	200	40	<500	0.9	< 100	< 100	<100
112-4	HIV-1_{MNp}	180	18	72 477	1.3	18 873	100	ND
113-4	HIV-1_{MNp}	180	40	70 667	0.3	4 947	653	32 163
112-1	HIV-1_{MNp}	180	40	<500	0.9	< 100	< 100	< 100
High-dose viral inoculation group								
136-3	HIV-1_{JRCSF}	65 000	25	252 381	0.8	958 871	1 797 600	232 155
136-2	HIV-1_{JRCSF}	65 000	29	50 167	0.7	41 172	54 521	8 600
141-1	HIV-1_{JRCSF}	65 000	30	67 667	2.2	27 735	52 430	429
161-3	HIV-1_{JRCSF}	65 000	30	13 847	0.9	104 466	14 653	111 080
157-3	HIV-1_{MNp}	20 000	31	1 253 925	0.5	41 053	56 802	976 556
157-4	HIV-1_{MNp}	20 000	31	147 973	0.6	3 634	262	40 796
161-6	HIV-1_{MNp}	20 000	31	108 073	1.7	4 991	< 100	3 673

Seven mice inoculated with a low infectious dose of HIV-1_{JRCSF} (200 $TCID_{50}$) or HIV-1_{MNp} (180 $TCID_{50}$), and 7 mice receiving a high infectious dose of HIV-1_{JRCSF} (65 000 $TCID_{50}$) or HIV-1_{MNp} (20 000 $TCID_{50}$) were listed.

ND indicates not done.

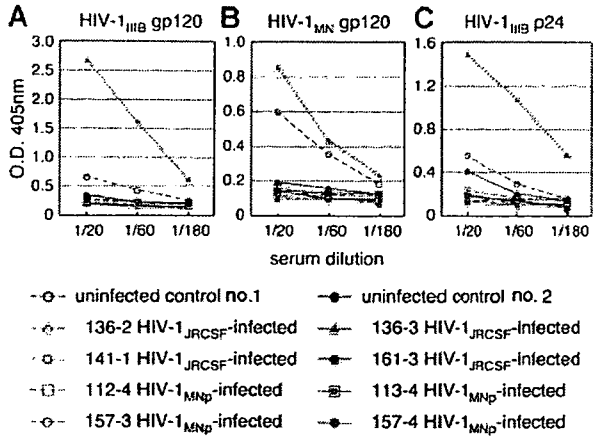

Figure 5. Detection of anti–HIV-1 antibodies from the plasma of HIV-1–infected mice. An ELISA assay was conducted by using plasma from 14 mice inoculated with either HIV-1_{JRCSF} or HIV-1_{MNp}, and from 2 uninfected control mice. Representatives (n = 8) of the 14 HIV-1–inoculated mice, and the 2 uninfected mice, are shown in the panels. Measurements of specific human antibodies for HIV-1_{IIIB} gp120 (A), HIV-1_{MN} gp120 (B), and HIV-1_{IIIB} p24 antigens (C) were shown. Results are expressed as the means from triplicate assays in 3 different experiments.

are initially activated in the xenogenic environment and then become anergic.[14] In contrast, SCID-hu (Thy/Liv) mice are more susceptible to X4 than to R5 strains[6] because HIV-1 infection is restricted mainly to the engrafted thymus that is primarily comprised of immature T cells, suggesting that this model may not be practical overt HIV infection. Our study represents the first attempt to infect NOG mice that received transplants of human hematopoietic stem cells with HIV-1. Very similar infection rates were seen for both R5 and X4 strains in the mouse model. Flow cytometry revealed both $CXCR4^+CD4^+$ and $CCR5^+CD4^+$ cells in PB, the spleen, and BM, but only CXCR4 on thymic $CD4^+$ T cells. It also showed the scattering of human macrophages, known to be susceptible to R5-tropic HIV-1 strains[28,29] and the source of HIV-1,[23,30-32] throughout various organs. $p24^+$ macrophage-like cells were detected in these organs after R5-tropic HIV-1_{JRCSF} infection. These data may help explain the susceptibility of hNOG mice to both R5- and X4-tropic HIV strains and also shed light on the active replenishment of these target cells in mice.

SCID mouse systems have been actively used in the evaluation of anti–HIV-1 drugs.[9,11,21] In most cases, HIV-1 detection levels reach a peak within a month after inoculation and level off, accompanied by $CD4^+$ T-cell depletion.[3,12,13] Although suitable for short-term experiments, it is also true that these models require large numbers of mice because of large variations in infection efficiency. In contrast, very stable infections were noted in our hNOG mice that were inoculated with a high dose of HIVs. They did not show rapid CD4/CD8 decrease in spite of high levels of viremia persisting for more than 40 days. Efficient hematopoiesis and thymopoiesis of human cells probably compensated for the loss of $CD4^+$ T cells, allowing for persistent infection. This capacity of the hNOG mouse system makes it attractive as a model for the long-term evaluation of anti–HIV-1 drugs. In addition to destroying mature blood cells, altered hematopoiesis in BM and the thymus has also been reported to be responsible for immunodeficiency in patients with AIDS.[33,34] To study hematopoietic abnormalities in HIV-1 infection, both SCID-hu (Thy/Liv) mice[8,35,36] and SIV- or SHIV-infected macaque models[20,37-39] have been used. The current hNOG mouse system, in which human cells are efficiently reproduced from stem cells and then settled into hematopoietic organs, offers a promising model for the study of events that occur after infection not only with R5-tropic HIV-1 but also with X4-tropic HIV-1. Indeed, the BM of hNOG mice infected with R5-tropic HIV-1 exhibited exceptionally elevated levels of HIV-DNA copies. On the other hand, the thymus of X4-tropic HIV-1_{MNp}–infected hNOG mice yielded large numbers of HIV-DNA copies, which seemed to correlate with the predominant expression of CXCR4 on the thymocytes. Thus, further observation is essential to address whether AIDS symptoms such as considerable $CD4^+$ T-cell depletion and hematopoietic abnormalities eventually occur in these mice.

It is noteworthy that human antibodies against both HIV-1 Env gp120 and Gag p24 antigens were detected in mice no. 136-3, no. 157-3, and no. 157-4 after exposure to high titers of HIV-1, suggesting that hNOG mice have the ability to respond to HIV-1 antigens. This encourages us to develop antibody-based HIV vaccine candidates, although additional modifications are required for the stable induction of immune responses. Importantly, since the seroconverted mice showed high viremia and high numbers of proviral DNA copies in the spleen, BM, and thymus, abundant viral production may stimulate human B-cell responses against HIV-1 and generate specific antibodies. These mice showed little or no detectable human IgG against HIV-1, as determined by Western blot analysis (data not shown), suggesting that very low levels of class-switching occurred in these mice, though further study is required.

In addition to the humoral immune responses, the induction of primary T-cell responses is critical for the study of HIV-specific immune responses and pathogenesis, as well as for vaccine development. Although we did not demonstrate the T-cell ability to respond to virus antigens, human T cells from the spleen proliferated when stimulated with anti–human CD3 antibodies (data not shown), indicating that the human T cells in the NOG mice that received transplants of hematopoietic stem cells are capable of responding to T-cell receptor–mediated signals and are expected to be able to elicit primary antigen-specific immune responses against foreign antigens. To address whether the specific T-cell responses may be induced will be one of the important studies.

In conclusion, the NOG mice that received transplants of human hematopoietic stem cells successfully achieved systemic and persistent infection with both R5-tropic and X4-tropic HIV-1, and generated humoral immune responses against HIV-1. These capacities of the hNOG mouse model may be very attractive for the study of HIV pathogenesis and humoral immune responses induced by HIV vaccine candidates.

Acknowledgments

We thank Yuetsu Tanaka of the University of Ryukyus, Tetsutaro Sata of NIID, and Shuzo Matsushita of Kumamoto University for their kind provision of mAbs to HIV-1, as well as Yukoku Tamaoka of Saiseikai Central Hospital, Toshio Akashi of Kumakiri Obstetric and Gynecologic Clinic, and Hideo Mugishima of Nihon University School of Medicine for their provision of umbilical cord blood. We also would like to express our gratitude to Ken Watanabe and Hideko Ogata of Tokyo Medical and Dental University for their skillful technical support.

This work was supported by grants from Research on Health Sciences focusing on Drug Innovation, the Japan Health Sciences Foundation.

Authorship

Contributions: S.W., K.T., N.S., M.H., and N.Y. designed the study; S.W., K.T., S.O., S.H., M.Y., Y.S., M.Z.D., and Z.Y. carried out the research; M.I. contributed live mice; S.W., K.T., and T.M. analyzed the data; N.S., M.H., and N.Y. controlled the data; S.W. wrote the paper; and all authors checked the final version of the manuscript.

Conflict-of-interest statement: The authors declare no competing financial interests.

Correspondence: Naoki Yamamoto, AIDS Research Center, National Institute of Infectious Diseases, 1-23-1 Toyama, Shinjuku-ku, Tokyo 162-8640, Japan; e-mail: nyama@nih.go.jp; Mitsuo Honda, AIDS Research Center, National Institute of Infectious Diseases, 1-23-1 Toyama, Shinjuku-ku, Tokyo 162-8640, Japan; e-mail: mhonda@nih.go.jp; and Norio Shimizu, Department of Virology, Division of Medical Science, Medical Research Institute, Tokyo Medical and Dental University, 1-5-45 Yushima, Bunkyo-ku, Tokyo 113-8519, Japan; e-mail: nshivir@tmd.ac.jp.

References

1. Letvin NL, Barouch DH, Montefiori DC. Prospects for vaccine protection against HIV-1 infection and AIDS. Annu Rev Immunol. 2002;20:73-99.
2. Namikawa R, Kaneshima H, Lieberman M, Weissman IL, McCune JM. Infection of the SCID-hu mouse by HIV-1. Science. 1988;242: 1684-1686.
3. Bonyhadi ML, Rabin L, Salimi S, et al. HIV induces thymus depletion in vivo. Nature. 1993; 363:728-732.
4. Aldrovandi GM, Feuer G, Gao L, et al. The SCID-hu mouse as a model for HIV-1 infection. Nature. 1993;363:732-736.
5. Su L, Kaneshima H, Bonyhadi M, et al. HIV-1-induced thymocyte depletion is associated with indirect cytopathogenicity and infection of progenitor cells in vivo. Immunity. 1995;2:25-36.
6. Kaneshima H, Su L, Bonyhadi ML, Connor RI, Ho DD, McCune JM. Rapid-high, syncytium-inducing isolates of human immunodeficiency virus type 1 induce cytopathicity in the human thymus of the SCID-hu mouse. J Virol. 1994;68:8188-8192.
7. Jenkins M, Hanley MB, Moreno MB, Wieder E, McCune JM. Human immunodeficiency virus-1 infection interrupts thymopoiesis and multilineage hematopoiesis in vivo. Blood. 1998;91:2672-2678.
8. Koka PS, Fraser JK, Bryson Y, et al. Human immunodeficiency virus inhibits multilineage hematopoiesis in vivo. J Virol. 1998;72:5121-5127.
9. Mosier DE, Gulizia RJ, Baird SM, Wilson DB, Spector DH, Spector SA. Human immunodeficiency virus infection of human-PBL-SCID mice. Science. 1991;251:791-794.
10. Torbett BE, Picchio G, Mosier DE. hu-PBL-SCID mice: a model for human immune function, AIDS, and lymphomagenesis. Immunol Rev. 1991;124: 139-164.
11. Ruxrungtham K, Boone E, Ford H Jr, Driscoll JS, Davey RT Jr, Lane HC. Potent activity of 2'-beta-fluoro-2',3'-dideoxyadenosine against human immunodeficiency virus type 1 infection in hu-PBL-SCID mice. Antimicrob Agents Chemother. 1996;40:2369-2374.
12. Mosier DE, Gulizia RJ, MacIsaac PD, Torbett BE, Levy JA. Rapid loss of CD4+ T cells in human-PBL-SCID mice by noncytopathic HIV isolates. Science. 1993;260:689-692.
13. Koyanagi Y, Tanaka Y, Kira J, et al. Primary human immunodeficiency virus type 1 viremia and central nervous system invasion in a novel hu-PBL-immunodeficient mouse strain. J Virol. 1997; 71:2417-2424.
14. Tary-Lehmann M, Saxon A, Lehmann PV. The human immune system in hu-PBL-SCID mice. Immunol Today. 1995;16:529-533.
15. Ito M, Hiramatsu H, Kobayashi K, et al. NOD/SCID/gamma(c)(null) mouse: an excellent recipient mouse model for engraftment of human cells. Blood. 2002;100:3175-3182.
16. Yahata T, Ando K, Nakamura Y, et al. Functional human T lymphocyte development from cord blood CD34+ cells in nonobese diabetic/Shi-scid, IL-2 receptor gamma null mice. J Immunol. 2002; 169:204-209.
17. Hiramatsu H, Nishikomori R, Heike T, et al. Complete reconstitution of human lymphocytes from cord blood CD34+ cells using the NOD/SCID/gammacnull mice model. Blood. 2003;102:873-880.
18. Matsumura T, Kametani Y, Ando K, et al. Functional CD5+ B cells develop predominantly in the spleen of NOD/SCID/gammac(null) (NOG) mice transplanted either with human umbilical cord blood, bone marrow, or mobilized peripheral blood CD34+ cells. Exp Hematol. 2003;31:789-797.
19. Shinohara K, Sakai K, Ando S, et al. A highly pathogenic simian/human immunodeficiency virus with genetic changes in cynomolgus monkey. J Gen Virol. 1999;80:1231-1240.
20. Yamakami K, Honda M, Takei M, et al. Early bone marrow hematopoietic defect in simian/human immunodeficiency virus C2/1-infected macaques and relevance to advance of disease. J Virol. 2004;78:10906-10910.
21. Nakata H, Maeda K, Miyakawa T, et al. Potent anti-R5 human immunodeficiency virus type 1 effects of a CCR5 antagonist, AK602/ONO4128/GW873140, in a novel human peripheral blood mononuclear cell nonobese diabetic-SCID, interleukin-2 receptor gamma-chain-knocked-out AIDS mouse model. J Virol. 2005;79:2087-2096.
22. Heath SL, Tew JG, Tew JG, Szakal AK, Burton GF. Follicular dendritic cells and human immunodeficiency virus infectivity. Nature. 1995;377:740-744.
23. Orenstein JM, Fox C, Wahl SM. Macrophages as a source of HIV during opportunistic infections. Science. 1997;276:1857-1861.
24. van Kooyk Y, Geijtenbeek TB. A novel adhesion pathway that regulates dendritic cell trafficking and T cell interactions. Immunol Rev. 2002;186: 47-56.
25. Taylor JR Jr, Kimbrell KC, Scoggins R, Delaney M, Wu L, Camerini D. Expression and function of chemokine receptors on human thymocytes: implications for infection by human immunodeficiency virus type 1. J Virol. 2001;75:8752-8760.
26. Bleul CC, Wu L, Hoxie JA, Springer TA, Mackay CR. The HIV coreceptors CXCR4 and CCR5 are differentially expressed and regulated on human T lymphocytes. Proc Natl Acad Sci U S A. 1997; 94:1925-1930.
27. Fais S, Lapenta C, Santini SM, et al. Human immunodeficiency virus type 1 strains R5 and X4 induce different pathogenic effects in hu-PBL-SCID mice, depending on the state of activation/differentiation of human target cells at the time of primary infection. J Virol. 1999;73:6453-6459.
28. Gartner S, Markovits P, Markovitz DM, Kaplan MH, Gallo RC, Popovic M. The role of mononuclear phagocytes in HTLV-III/LAV infection. Science. 1986;233:215-219.
29. Koyanagi Y, Miles S, Mitsuyasu RT, Merrill JE, Vinters HV, Chen IS. Dual infection of the central nervous system by AIDS viruses with distinct cellular tropisms. Science. 1987;236:819-822.
30. Gendelman HE, Orenstein JM, Baca LM, et al. The macrophage in the persistence and pathogenesis of HIV infection. AIDS. 1989;3:475-495.
31. Embretson J, Zupancic M, Ribas JL, et al. Massive covert infection of helper T lymphocytes and macrophages by HIV during the incubation period of AIDS. Nature. 1993;362:359-362.
32. Igarashi T, Brown CR, Endo Y, et al. Macrophage are the principal reservoir and sustain high virus loads in rhesus macaques after the depletion of CD4+ T cells by a highly pathogenic simian immunodeficiency virus/HIV type 1 chimera (SHIV): implications for HIV-1 infections of humans. Proc Natl Acad Sci U S A. 2001;98:658-663.
33. Mir N, Costello C, Luckit J, Lindley R. HIV-disease and bone marrow changes: a study of 60 cases. Eur J Haematol. 1989;42:339-343.
34. Moses A, Nelson J, Bagby GC Jr. The influence of human immunodeficiency virus-1 on hematopoiesis. Blood. 1998;91:1479-1495.
35. Koka PS, Jamieson BD, Brooks DG, Zack JA. Human immunodeficiency virus type 1-induced hematopoietic inhibition is independent of productive infection of progenitor cells in vivo. J Virol. 1999;73:9089-9097.
36. Koka PS, Kitchen CM, Reddy ST. Targeting c-Mpl for revival of human immunodeficiency virus type 1-induced hematopoietic inhibition when CD34+ progenitor cells are re-engrafted into a fresh stromal microenvironment in vivo. J Virol. 2004;78: 11385-11392.
37. Hillyer CD, Lackey DA 3rd, Villinger F, Winton EF, McClure HM, Ansari AA. CD34+ and CFU-GM progenitors are significantly decreased in SIVsmm9 infected rhesus macaques with minimal evidence of direct viral infection by polymerase chain reaction. Am J Hematol. 1993;43:274-278.
38. Thiebot H, Louache F, Vaslin B, et al. Early and persistent bone marrow hematopoiesis defect in simian/human immunodeficiency virus-infected macaques despite efficient reduction of viremia by highly active antiretroviral therapy during primary infection. J Virol. 2001;75:11594-11602.
39. Thiebot H, Vaslin B, Derdouch S, et al. Impact of bone marrow hematopoiesis failure on T-cell generation during pathogenic simian immunodeficiency virus infection in macaques. Blood. 2005; 105:2403-2409.

Brief report

Somatic revertant mosaicism in a patient with leukocyte adhesion deficiency type 1

Yumi Tone,[1] Taizo Wada,[1] Fumie Shibata,[1] Tomoko Toma,[1] Yoko Hashida,[1] Yoshihito Kasahara,[1] Shoichi Koizumi,[1] and Akihiro Yachie[2]

[1]Department of Pediatrics, Graduate School of Medical Science and School of Medicine, Kanazawa University, Kanazawa, Japan; and [2]Department of Laboratory Sciences, School of Health Sciences, Faculty of Medicine, Kanazawa University, Kanazawa, Japan

Leukocyte adhesion deficiency type 1 (LAD-1) is an autosomal recessive disorder caused by mutations in the *ITGB2 (CD18)* gene and characterized by recurrent severe infections, impaired pus formation, and defective wound healing. We describe an unusual case of severe phenotypic LAD-1 presenting with somatic mosaicism. The patient is a compound heterozygote bearing 2 different frameshift mutations that abrogate protein expression. However, CD18 expression was detected in a small proportion of T cells but was undetectable in granulocytes, monocytes, B cells, and natural killer (NK) cells. The T cells were not of maternal origin, lacked the paternal mutation, and showed a selective advantage in vivo. Molecular analysis using sorted CD18$^+$ cells revealed them to be derived from a single CD8$^+$ T cell carrying T-cell receptor VB22. These findings suggest that spontaneous in vivo reversion was responsible for the somatic mosaicism in our patient. (Blood. 2007;109:1182-1184)

Introduction

Leukocyte adhesion deficiency type 1 (LAD-1) is an autosomal recessive immunodeficiency disorder characterized by recurrent bacterial infections, impaired pus formation, and defective wound healing.[1,2] The disease gene, *ITGB2*, is located on 21q22.3 and encodes the common chain of the β_2 integrin family, CD18.[1,2] Integrins are cell membrane receptors composed of α and β subunits that mediate adhesion events in all tissues, and β_2 integrins are expressed only on leukocytes as heterodimers with an α chain (CD11a/CD18, CD11b/CD18, CD11c/CD18). Patients with LAD-1 are therefore uniformly deficient in the expression of all 3 leukocyte integrins.[1,2]

Somatic mosaicism as a result of in vivo reversion has recently been increasingly reported in patients affected with primary immunodeficiencies.[3] The resultant effects on clinical phenotype range from milder manifestations characterized as natural gene therapy to none.[3] Thus, the potential clinical consequences of revertant mosaicism remain difficult to predict. Here, we describe an unusual case of LAD-1 with a mosaic pattern of CD18 expression and elucidate the nature of the reversion and its effects on revertant cells and clinical features.

Patient, materials, and methods

Patient

The patient was the first child of nonconsanguineous, healthy Japanese parents. At 1 day of age he developed omphalitis as a result of group B streptococcus and was successfully treated with intravenous antibiotics. The umbilical cord was separated at 17 days. At 2 months of age he had an infected urachal cyst that required antibiotics and surgical excision. Because of delayed wound healing and persistent leukocytosis (22.5-48.2 × 10^9/L), he was referred to our hospital at age 3 months. Fluorescence-activated cell sorting (FACS) analysis demonstrated the absence of CD18 (Figure 1A) and its associated molecules CD11b and CD11c (data not shown) on his granulocytes and monocytes. On the basis of these findings a diagnosis of LAD-1 was made. Despite prophylactic antibiotics, recurrent perianal cellulitis was noted from 5 months of age. The patient has not received any blood product transfusion.

Molecular and cellular studies

CD18$^+$ cells were enriched from peripheral blood mononuclear cells (PBMCs) using magnetic beads (BD PharMingen, San Diego, CA). Microsatellite polymorphic markers, including D9S1198, the human androgen receptor gene, and the heme oxygenase-1 promoter, were amplified with FAM-labeled specific primers[4,5] and subjected to GeneScan analysis.[6] Mutation analysis of the *ITGB2* gene, FACS analysis of T-cell receptor (TCR) VB repertoire, and complementarity-determining region 3 (CDR3) spectratyping were performed as described elsewhere.[7-9] CD8$^+$ T cells were examined for CD69 and CD25 expression by 3-color FACS analysis after incubation for 16 hours with a combination of 5 μg/mL anti-CD2 monoclonal antibodies (mAbs; Beckman Coulter, Fullerton, CA), alone or together with 100 U/mL interleukin-2 or 5 μg/mL anti-CD28 mAb (BD PharMingen).[10] Approval for the study was obtained from the Human Research Committee of Kanazawa University Graduate School of Medical Science, and informed consent was provided according to the Declaration of Helsinki.

Results and discussion

The clinical features of our patient were consistent with a severe form of LAD-1. Direct genomic sequence analysis of granulocytes showed him to be a compound heterozygote for 2 different mutations. One was a splice site mutation, G>A (+1), intron 4, that caused exon 4 skipping; the other was a single C deletion

Submitted August 1, 2006; accepted September 8, 2006. Prepublished online as *Blood* First Edition Paper, September 21, 2006; DOI 10.1182/blood-2006-08-039057.

The publication costs of this article were defrayed in part by page charge payment. Therefore, and solely to indicate this fact, this article is hereby marked "advertisement" in accordance with 18 USC section 1734.

following nucleotides 670 to 674 in exon 6, both of which resulted in frameshift and affected the highly conserved domain (exons 5 through 9) of CD18 (Figure 1C). The parents were heterozygous carriers. These novel mutations should have led to the complete absence of biosynthesis of the β_2 subunit of leukocyte integrins. However, a small proportion of the patient's lymphocytes were CD18$^+$ (Figure 1A). To determine the lymphocyte population responsible for CD18 expression, multicolor FACS analysis was performed. As shown in Figure 1B, CD18$^+$ cells were found to include CD8$^+$ T cells but were not detected among CD4$^+$ T, CD20$^+$ B, or CD56$^+$ natural killer (NK) cells. The CD18$^+$CD8$^+$ T cells expressed significant levels of CD57 but not CD28, indicating a memory/effector phenotype.

To assess whether the same mutations were present in the patient's CD18$^+$ T cells, sequencing analysis was performed on genomic DNA obtained from enriched CD18$^+$ T cells. The purity of the enriched cells was about 80%, as determined by FACS analysis. As shown in Figure 1C, we found that the patient's CD18$^+$ T cells lacked the splice site mutation in intron 4, although a minor peak of nucleotide A originating from contaminating CD18$^-$ cells was also seen at the position of the mutation. Molecular typing of the enriched CD18$^+$ T cells using 3 different polymorphic markers showed that they were not derived from maternal T-cell engraftment (Figure 1D). We therefore conclude that the patient's CD18$^+$ T cells result from site-specific single nucleotide reversion of the inherited paternal mutation.

FACS analysis of the TCR VB repertoire clearly demonstrated that the patient's CD18$^+$ T cells were detectable only with TCR VB22 (Figure 1E). Analysis of CDR3 spectratyping and the junctional amino acid sequence of TCR VB22 also showed a monoclonal CD18$^+$ T-cell profile (Figure 1F; Table 1). Taken together, these findings suggest that the reversion of the paternal mutation occurred in a committed CD8$^+$ T cell in the patient and that mature hematopoietic cells as well as early progenitors[3] could be the elements in which the in vivo reversion occurred. In addition, the accumulation of CD18$^+$ T cells to levels that reached the detection threshold of FACS analysis suggests that CD18$^+$ T cells might have a selective growth advantage in vivo over CD18$^-$ cells. Indeed, in canine LAD models, following nonmyeloablative hematopoietic stem cell transplantation, the extent of donor chimerism was greater in peripheral T cells than in neutrophils and monocytes and increased progressively over time.[11]

T-cell activation mediated by a combination of anti-CD2 mAbs that react with T11.1 or T11.2 epitopes is severely defective in patients with LAD.[10] To evaluate the functionality of CD18$^+$CD8$^+$ T cells we examined the surface expression of activation markers after incubation with anti-CD2 mAbs. As shown in Figure 1G, CD69 and CD25 expression on the patient's CD18$^-$CD8$^+$ T cells was impaired. In contrast, the revertant CD18$^+$CD8$^+$ T cells showed significantly improved responses to anti-CD2 stimulation, indicating that the genetic reversion had led to reversal of the biologic defects characteristic of LAD T cells. The severity of

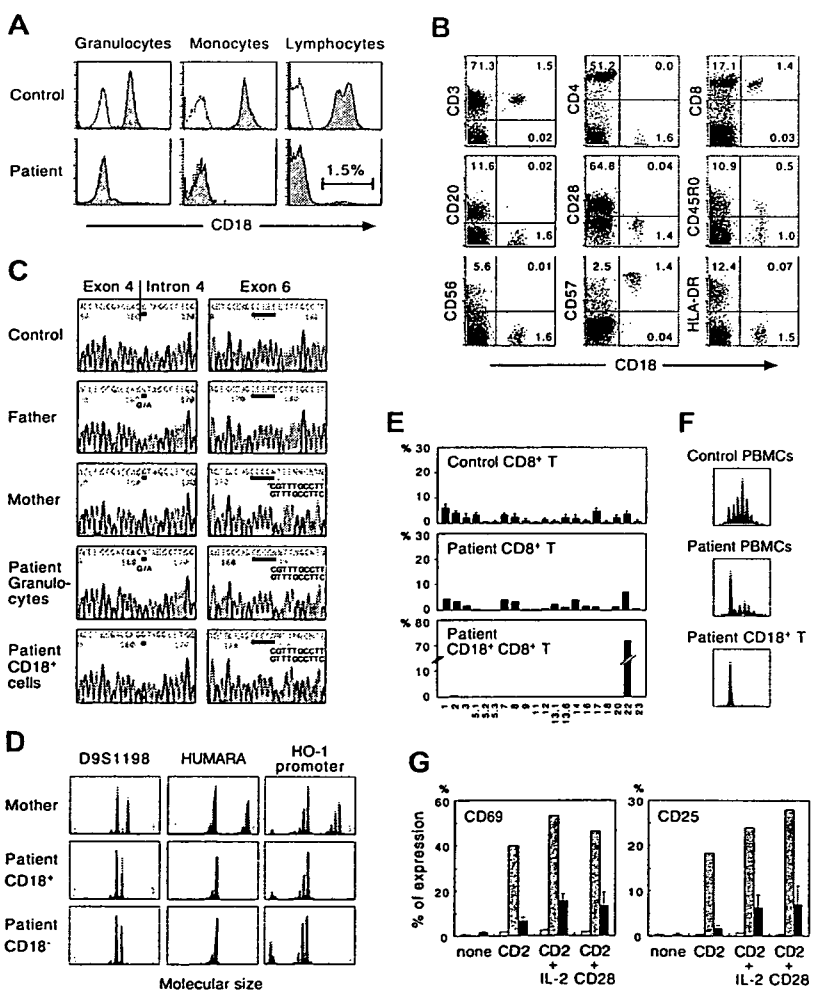

Figure 1. Characterization of CD18 expression, *ITGB2* gene mutations, T-cell receptor repertoire, and T-cell functions. (A) Analysis of CD18 expression. Shown are the results of CD18 expression on granulocytes, monocytes, and lymphocytes. Open peaks indicate control Ab; solid peaks represent anti-CD18 mAb. (B) CD18 expression on the patient's lymphocyte subsets. The percentage of cells gated in each quadrant is shown. (C) Mutation analysis. The *ITGB2* gene was amplified from DNA extracted from normal PBMCs, PBMCs from the parents, and the patient's granulocytes and CD18$^+$ T cells. Direct sequencing was performed using an automated sequencer. Bars show the locations of the mutations. (D) Microsatellite analysis. Three different markers were amplified with FAM-labeled specific primers and subjected to GeneScan analysis. HUMARA indicates human androgen receptor gene; HO-1, heme oxygenase-1. (E) Expression profiles of TCR VB subfamilies. Peripheral blood samples were stained with mAbs for individual TCR VB subfamilies together with anti-CD8 and anti-CD18 mAbs. The expression of each TCR VB by CD8$^+$ or CD18$^+$CD8$^+$ T cells was analyzed by FACS. (F) CDR3 spectratyping. A TCR VB22 fragment was amplified from cDNA with specific primers. The size distribution of polymerase chain reaction products was determined by GeneScan analysis. (G) Analysis of CD2-mediated T-cell activation. PBMCs from healthy control subjects and the patient were cultured for 16 hours with a combination of anti-CD2 mAbs alone or together with interleukin-2 or anti-CD28 mAb. CD69 and CD25 expression was evaluated in the patient's CD18$^-$CD8$^+$ T (□) and CD18$^+$CD8$^+$ T (▤) cells. ■ indicate control CD8$^+$ T cells from healthy adults. Error bars represent SD.

Table 1. Junctional amino acid sequences of TCR VB22

BV	N-D-N	BJ	Frequency*
Normal PBMCs			
CASS	EWGF	TDTQYFGPGTRLTVL	2/18
CASS	ELVRA	NSPLHFGNGTRLTVT	2/18
CAS	TEGTGV	YNEQFFGPGTRLTVL	2/18
CASS	FRV	HEQYFGPGTRLTVT	1/18
CAI	ATGA	SYEQYFGPGTRLTVT	1/18
CASS	RSTGLSD	SGANVLTFGAGSRLTVL	1/18
CAS	RRTG	ETQYFGPGTRLLVL	1/18
CAS	TDRGA	NTGELFFGEGSRLTVL	1/18
CASS	EP	YEQYFGPGTRLTVT	1/18
CAS	GGDHV	TDTQYFGPGTRLTVL	1/18
CASS	ELI	TDTQYFGPGTRLTVL	1/18
CAS	RGTVT	YNEQFFGPGTRLTVL	1/18
CASS	AGSM	NTEAFFGQGTRLTVV	1/18
CASS	EGGGG	TEAFFGQGTRLTVV	1/18
CASS	EALQGALN	EQYFGPGTRLTVT	1/18
Patient CD18⁺ T cells			
CASS	PD	NEQFFGPGTRLTVL	24/24

*Number of each clone in the total cDNA clones characterized.

clinical features in patients with LAD-1 is directly related to the degree of CD18 deficiency. Patients with less than 1% residual expression of β_2 integrins have the severe form of LAD-1, whereas those with 1% to 10% expression show a moderate phenotype.[1] Our patient, however, has shown no improvement in clinical symptoms as a consequence of the revertant mosaicism, probably because no reversion events occurred in myeloid cells. These findings and previous observations[6,9] suggest that the clinical consequences of reversion may depend on cell lineage, size and diversity, and the functional restoration of revertant cells.

In summary, our results provide an additional example of genetic reversion in a primary immunodeficiency and further support the possibility that somatic revertant mosaicism could be present in any genetic disorder in which revertant cells have a selective growth advantage in vivo but remain undetected because they do not necessarily result in modification of the clinical phenotype.

Acknowledgments

We thank Ms Harumi Matsukawa and Ms Mika Tamamura for excellent technical assistance.

This work was supported by a Grant-in-Aid for Scientific Research from the Ministry of Education, Culture, Sports, Science, and Technology of Japan and a grant from the Ministry of Health, Labour, and Welfare of Japan, Tokyo.

Authorship

Contribution: Y.T., T.W., and A.Y. participated in designing and performing the research; F.S., T.T., Y.H., Y.K., and S.K. analyzed the data; Y.T. and T.W. wrote the paper; and all authors checked the final version of the manuscript.

Conflict-of-interest disclosure: The authors declare no competing financial interests.

Correspondence: Taizo Wada, Department of Pediatrics, Graduate School of Medical Science, Kanazawa University, 13-1 Takaramachi, Kanazawa 920-8641, Japan; e-mail: taizo@ped.m.kanazawa-u.ac.jp.

References

1. Anderson DC, Smith CW. Leukocyte adhesion deficiencies. In: Scriver CR, Beaudet AL, Sly WS, Valle D, eds. The Metabolic and Molecular Bases of Inherited Disease. Vol III. New York, NY: McGraw-Hill; 2001:4829-4856.
2. Bunting M, Harris ES, McIntyre TM, Prescott SM, Zimmerman GA. Leukocyte adhesion deficiency syndromes: adhesion and tethering defects involving β2 integrins and selectin ligands. Curr Opin Hematol. 2002;9:30-35.
3. Hirschhorn R. In vivo reversion to normal of inherited mutations in humans. J Med Genet. 2003;40: 721-728.
4. Niida Y, Stemmer-Rachamimov AO, Logrip M, et al. Survey of somatic mutations in tuberous sclerosis complex (TSC) hamartomas suggests different genetic mechanisms for pathogenesis of TSC lesions. Am J Hum Genet. 2001;69:493-503.
5. Kimpara T, Takeda A, Watanabe K, et al. Microsatellite polymorphism in the human heme oxygenase-1 gene promoter and its application in association studies with Alzheimer and Parkinson disease. Hum Genet. 1997;100:145-147.
6. Wada T, Konno A, Schurman SH, et al. Second-site mutation in the Wiskott-Aldrich syndrome (WAS) protein gene causes somatic mosaicism in two WAS siblings. J Clin Invest. 2003;111:1389-1397.
7. Roos D, Meischl C, de Boer M, et al. Genetic analysis of patients with leukocyte adhesion deficiency: genomic sequencing reveals otherwise undetectable mutations. Exp Hematol. 2002;30: 252-261.
8. Mizuno K, Yachie A, Nagaoki S, et al. Oligoclonal expansion of circulating and tissue-infiltrating CD8⁺ T cells with killer/effector phenotypes in juvenile dermatomyositis syndrome. Clin Exp Immunol. 2004;137:187-194.
9. Wada T, Toma T, Okamoto H, et al. Oligoclonal expansion of T lymphocytes with multiple second-site mutations leads to Omenn syndrome in a patient with RAG1-deficient severe combined immunodeficiency. Blood. 2005;106:2099-2101.
10. Kuijpers TW, Van Lier RA, Hamann D, et al. Leukocyte adhesion deficiency type 1 (LAD-1)/variant: a novel immunodeficiency syndrome characterized by dysfunctional β2 integrins. J Clin Invest. 1997;100:1725-1733.
11. Bauer TR Jr, Creevy KE, Gu YC, et al. Very low levels of donor CD18⁺ neutrophils following allogeneic hematopoietic stem cell transplantation reverse the disease phenotype in canine leukocyte adhesion deficiency. Blood. 2004;103:3582-3589.

Clinical Immunology (2007) 125, 237 246

available at www.sciencedirect.com

ScienceDirect

www.elsevier.com/locate/yclim

Developmental changes of FOXP3-expressing CD4$^+$CD25$^+$ regulatory T cells and their impairment in patients with *FOXP3* gene mutations

Tatsuya Fuchizawa [a], Yuichi Adachi [a,*], Yasunori Ito [a], Hiroyuki Higashiyama [a], Hirokazu Kanegane [a], Takeshi Futatani [a], Ichiro Kobayashi [b], Yoshiro Kamachi [c], Tatsuo Sakamoto [c], Ikuya Tsuge [d], Hiroshi Tanaka [e], Alison H. Banham [f], Hans D. Ochs [g], Toshio Miyawaki [a]

[a] *Department of Pediatrics, Graduate School of Medicine, University of Toyama, 2630 Sugitani, Toyama, Toyama 930-0194, Japan*
[b] *Pediatric Clinic, Kitami Red Cross General Hospital, Kitami, Japan*
[c] *Department of Pediatrics, Nagoya University Graduate School of Medicine, Nagoya, Japan*
[d] *Department of Pediatrics, Fujita Health University School of Medicine, Toyoake, Japan*
[e] *Department of Pediatrics, Hirosaki University School of Medicine, Hirosaki, Japan*
[f] *Nuffield Department of Clinical Laboratory Sciences, University of Oxford, Oxford, UK*
[g] *Department of Pediatrics, University of Washington School of Medicine, Seattle, WA, USA*

Received 11 May 2007; accepted with revision 8 August 2007
Available online 3 October 2007

KEYWORDS
FOXP3;
Regulatory T cells;
Developmental change;
Naive T cells;
Memory T cells;
IPEX

Abstract FOXP3 is required for the generation and function of CD4$^+$CD25$^+$ regulatory T (Treg) cells. To elucidate the biological role of Treg cells, we used a monoclonal anti-FOXP3 antibody to examine the frequencies of Treg cells during child development. The percentages of CD4$^+$CD25$^+$FOXP3$^+$ T cells were constant shortly from after birth through adulthood. CD4$^+$CD25$^+$FOXP3$^+$ T cells in cord blood showed the naive CD45RA$^+$CD45RO$^-$ phenotype, whereas adult CD4$^+$CD25$^+$FOXP3$^+$ T cells expressed mostly the memory CD45RA$^-$CD45RO$^+$ phenotype. The age-dependent dominance of memory CD4$^+$CD25$^+$FOXP3$^+$ T cells implies functional differences between naive and memory Treg cells. Notably, four patients with *FOXP3* gene mutations revealed a paucity of CD4$^+$CD25$^+$FOXP3$^+$ T cells. Importantly, one patient with a frame shift mutation, who showed typical symptoms of IPEX (immune dysregulation, polyendocrinopathy, enteropathy, X-linked), exhibited marked T cell activation, whereas others with missense mutations, who were clinically milder, did not. This observation suggests a possible genotype phenotype correlation in IPEX.

* Corresponding author. Fax: +81 76 434 5029.
E-mail address: yadachi@med.u-toyama.ac.jp (Y. Adachi).

1521-6616/$ see front matter © 2007 Elsevier Inc. All rights reserved.
doi:10.1016/j.clim.2007.08.004

Introduction

$CD4^+CD25^+$ regulatory T (Treg) cells represent a unique lineage of immunoregulatory cells both in humans and animals, and play a central role in the maintenance of immunological self-tolerance [1,2]. In addition, Treg cells were shown to exert a suppressive function on the immune responses to various self and nonself antigens, alloantigens, external antigens, and tumor antigens [3 5]. These observations provide new insights into the immunopathogenesis of human diseases, such as autoimmune and allergic diseases, malignances, and complications of bone marrow or organ transplantation.

Most recently, forkhead box P3 (*FOXP3*) has emerged as a master control gene for the generation and function of Treg cells [6,7], as illustrated by the demonstration that naturally occurring defects in FOXP3 cause characteristic autoimmune syndrome in mice and humans [8 11]. Failure to properly regulate $CD4^+$ effector T cells, caused by lack of $CD4^+CD25^+FOXP3^+$ Treg cells, is directly responsible for the X-linked scurfy syndrome (*sf*) in mice [12], characterized by early-onset lymphohistiocytic infiltrates of the skin and lymphoid organs, severe runting secondary to chronic diarrhea, and hypergammaglobulinemia. The human orthologue, immune dysregulation, polyendocrinopathy, enteropathy, X-linked (IPEX) is a rare inborn error characterized by the early onset of multiple autoimmune diseases [13]. It has been shown that FOXP3 is expressed mainly in a subset of $CD4^+CD25^+$ T cells which correlates with the suppressive activity of regulatory T cells [7]. Retroviral gene transfer of *FOXP3* converts naive T cells into a phenotype similar to that of naturally occurring Treg cells [6]. Thus, FOXP3 expression is used as a surrogate molecular marker for quantifying Treg cells in the peripheral blood.

Whether Treg cells are exclusively generated in the thymus or may differentiated from peripheral $CD4^+CD25^+$ naive T cells is controversial. *In vitro* activation of human $CD4^+CD25^-$ T cells through T cell receptor stimulation was shown by some investigators to induce FOXP3 expression and suppressor function similar to freshly isolated $CD4^+CD25^+$ T cells [14,15], but not by others [16]. In the peripheral blood of healthy adults, the majority of Treg cells, identified as $CD4^+CD25^+FOXP3^+$ T cells, were shown to have the memory $CD45RA^-CD45RO^+$ phenotype [17]. Recently, it has been reported that human $CD4^+CD45RO^+CD25^{hi}FOXP3^+$ T cells are susceptible to apoptosis and have limited self-renewal capacity, suggesting that conversion of CD25-negative to CD25-positive memory T cells in the periphery is one of the pathways for the generation of Treg cells [18]. In contrast, $CD4^+CD25^+FOXP3^+$ T cells in cord blood appear to essentially show the naive $CD45RA^+CD45RO^-$ phenotype [19]. However, a small number of Treg cells of the naive phenotype have been identified in the peripheral blood of adults; their frequency seems to decrease with age [20,21]. In this study, we explored the quantity of circulating Treg cells during childhood development in order to understand better the potential immunopathogenesis of human diseases resulting from dysregulated peripheral tolerance. Using flow cytometric analysis and an anti-FOXP3 monoclonal antibody (mAb), we examined how FOXP3-expressing $CD4^+CD25^+$ T cells of the naive and memory phenotypes might change from birth to adulthood. We also analyzed FOXP3 expression in IPEX patients to study the effect of different mutations of *FOXP3* gene on the generation of Treg cells.

Subjects, materials, and methods

Subjects

Venous blood samples were obtained from children of various ages and adult volunteers at the Toyama University Hospital. Individuals with allergic or autoimmune diseases, malignancies, hematologic disorders, or acute infections were excluded. Cord blood samples were obtained from the placentas of full-term newborns at Okada Obstetrics and Gynecology Hospital, who did not have hereditary disorders, hematologic abnormalities, or infectious complications. The total number of samples was 147 and consisted of 12 cord bloods, and samples from 36 newborn infants, 78 children (1 18 years old), and 21 adults (19 44 years old). Blood samples were obtained from four IPEX patients with *FOXP3* gene mutations. The clinical characteristic and *FOXP3* gene mutations are summarized in Table 1. Clinical manifestations are variable, with two patients requiring immunosuppressive therapy. Patient 1 and 4 have been reported previously [22,23]. Patient 1 had a family history of affected males reporting early onset of severe polyautoimmunity. Patient 2 and 3 were siblings. All samples were obtained after informed consent was obtained; the study was approved by the University of Toyama ethics committee.

Flow cytometric analysis and antibodies used

Mononuclear cells (MNC) were isolated from heparinized blood by density gradient centrifugation over Histopaque-1077 (Sigma-Aldrich, Inc., St. Louis, MO). FOXP3 expression was analyzed by flow cytometry according to the protocol described previously [24]. Briefly, fresh MNC were washed in PBS, fixed in 1 ml of PBS with 1% paraformaldehyde and 0.05% Tween-20, and kept overnight at 4 °C. Cells were treated twice with 0.5 ml of DNAse 100 Kunitz units/ml according to the manufacturer s instructions (Sigma-Aldrich, Inc.). Cells were incubated with a murine anti-human-FOXP3 mAb (clone150D/E4), previously described [24], for 1 h at room temperature, washed with FACS buffer (PBS, 3.0% fetal calf serum, 0.5% Tween-20, and 0.05% azide). FOXP3 staining was detected using Alexa Fluor-488 goat anti-mouse-IgG antibody (Molecular Probes; Invitrogen, Eugen, OR) and washed as described above. Cell surface staining was then performed using PC5-conjugated anti-human-CD4 (Immunotech, Marseille, France) and PE-conjugated anti-human-CD25 (Miltenyi Biotec, Bergish Gladbach, Germany) mAbs for 20 min at room temperature. Cells were analyzed using a flow cytometer (EPICS XL-MCL; Beckman Coulter KK, Tokyo, Japan).

For phenotypic analysis, fresh MNC were stained with a combination of the following antibodies: PE-conjugated anti-CD3 (Dako Japan, Kyoto, Japan), FITC-conjugated anti-HLA-DR (Immunotech), PE-conjugated anti-CD4 (Dako Japan), PE-conjugated anti-CD8 (Dako Japan), FITC-conjugated anti-CD45RO (Dako Japan), ECD-conjugated anti-CD45RA (Immunotech), FITC-conjugated anti-CD19 (Dako Japan), and PE-conjugated anti-CD56 (Immunotech) mAbs.

Table 1 Clinical findings and *FOXP3* mutations of patients with IPEX

	Patient 1 [22][a]	Patient 2 brother of 3	Patient 3 brother of 2	Patient 4 [23]
Age at onset	5 days	2 months	19 days	2 months
Present age	15 years	6 years	15 years	3 years
Family history	Positive	Positive	Positive	Negative
Gene mutation	227delT	1150G>A	1150G>A	1117T>G
	Frame shift	Ala384Thr	Ala384Thr	Phe373Val
	Novel mutation	Reported mutation	Reported mutation	Novel mutation
Initial presentations	Autoimmune thyroiditis	Atopic dermatitis	Eosinophilic gastroenteritis	Autoimmune enteropathy
		Failure to thrive		
Other manifestations	Autoimmune hemolytic anemia	Bronchial asthma	Atopic dermatitis	No other autoimmune diseases
	Autoimmune enteropathy	Adrenal dysfunction		
	Renal tubular dysfunction			
	Osteoporosis			
Growth retardation	Severe	Moderate	None	None
Therapy	Tacrolimus, bethamethasone	Inhaled steroid	None	Cyclosporin, IVIG

IVIG: intravenous immunoglobulin.
[a] Indicates number of reference that reports a patient.

Statistical analysis

The statistical significance of differences was determined with Student s *t* test. *P* values <0.05 were considered significant.

Results

FOXP3-expressing lymphocytes

Flow cytometric analysis using a murine anti-human FOXP3 mAb revealed that FOXP3 expression, at any age, was detectable mainly within the CD4+CD25+ T cell population and only rarely in CD4+CD25− T cells (Fig. 1). Few CD8+ T, B, and NK cells expressed FOXP3 (data not shown). Table 2 summarizes the frequency of CD25+FOXP3+ cells within the CD4+ T cell population at various ages. We found that the percentages of CD25+FOXP3+ cells within CD4+ T cells in cord blood were significantly lower than those in adults. Importantly, the percentage of CD4+CD25+FOXP3+ T cells in the peripheral blood reached normal adult levels shortly after birth, and the frequency of FOXP3+CD25+ cells within CD4+ T cells appeared to be relatively stable until adulthood (Table 2). In contrast to CD4+CD25+FOXP3+ T cells, the percentages of total CD25+ cells within CD4+ T cells increased with age during the first three years of life, presumably reflecting an accumulation over time of recently activated CD4+ T cells in the blood. After reaching a plateau at age 12, total CD25+ cells within CD4+ T cells did not change through adulthood.

Phenotyping of FOXP3-expressing CD4+CD25+ T cells

Human naive and memory T cells can be distinguished by the reciprocal expression of CD45RA and CD45RO isoforms. It has been observed that CD4+CD25+ T cells in cord blood have mainly the naive CD45RA+CD45RO− phenotype [19], whereas those in adult blood show the memory CD45RA−CD45RO+ phenotype [17]. We examined expression of CD45RA and CD45RO isoforms by CD4+CD25+ T cells in children of various age and in adult donors (Fig. 2A). In accord with previous observations, we found that CD25+ cells in cord blood were predominantly present in the CD45RA+CD45RO−CD4+ T cell population. In adults, most CD4+CD25+ T cells expressed CD45RO, while a minority of them expressed CD45RA. As expected, an age-dependent increase of CD4+CD25+ T cells with the memory phenotype (CD45RO) and a decrease of the percentages of CD4+CD25+ T cells with the naive phenotype (CD45RA) were observed (Fig. 2B).

We then examined the expression of the CD45RA and CD45RO isoforms by FOXP3-expressing CD4+CD25+ T cells in children of various ages and in adults (Fig. 3). Although the frequency of FOXP3-expressing CD4+CD25+ T cells was relatively stable from birth until adulthood (Table 2), the expression profiles of CD45 isoforms by FOXP3-expressing CD4+CD25+ T cell cells dynamically changed with age. As can be seen in Fig. 3, CD4+CD25+FOXP3+ T cells expressing CD45RA predominate in infants and decrease during childhood with a concomitant increase of the CD45RO-positive fraction in the CD4+CD25+FOXP3+ T cell population. Thus, the vast majority of adult CD4+CD25+FOXP3+ T cells express the CD45RO-isotype, with very few expressing CD45RA.

FOXP3 expression in patients with IPEX

We next examined FOXP3 expression in four IPEX patients with *FOXP3* gene mutations to ask whether their mutations might result in the absence of FOXP3, presumably leading to a deficit of Treg cells. As shown in Fig. 4A, expression of FOXP3 by CD4+ T cells was remarkably reduced in all

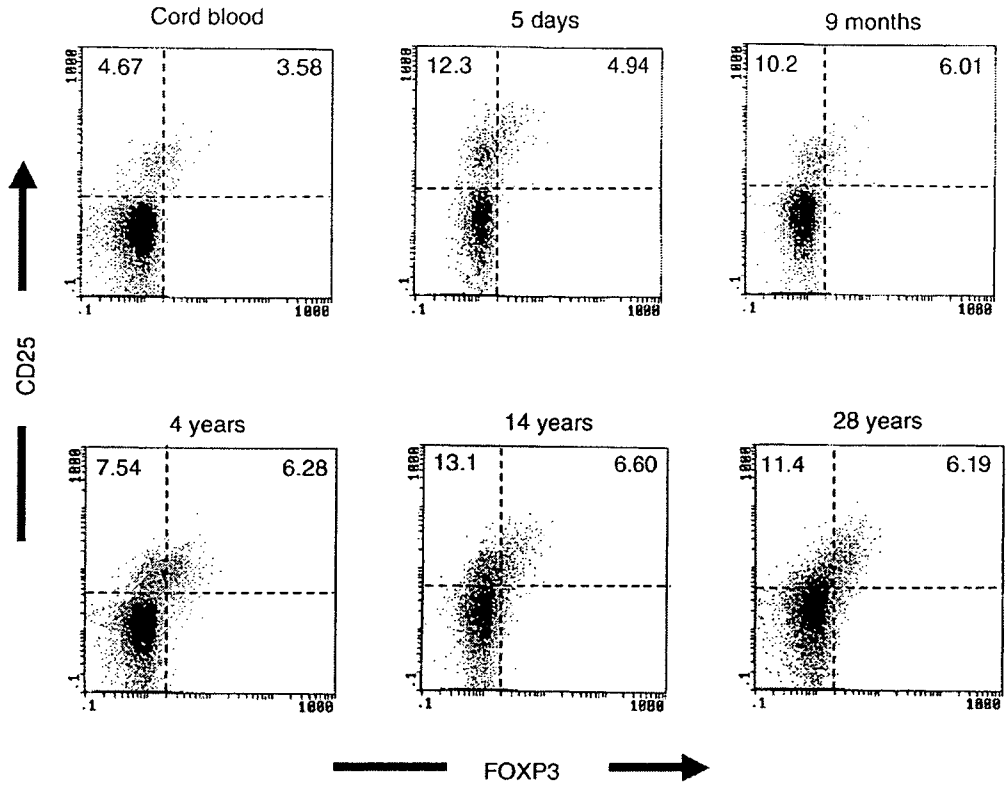

Figure 1 Flow cytometric analysis of FOXP3 expression in circulating $CD4^+$ T cells of different age groups. MNC were stained simultaneously for CD4, FOXP3, and CD25, and analyzed by flow cytometry for the expression of FOXP3 and/or CD25. The numbers in each quadrant indicate percentages of the respective subpopulation.

patients. The percentages of $CD4^+CD25^+FOXP3^+$ T cells were less than 1% of $CD4^+$ cells in all patients (Table 3), whereas normal individuals had approximately 5% of this type of cells (Table 2). Notably, $CD25^{bright}CD4^+$ T cells were absent in the patients when compared with normal controls (Fig. 1). Patient 1 had more $CD4^+CD25^+$ cells than normal subjects, although their CD25 expression was dim or intermediate. The other patients showed lower percentages of $CD4^+CD25^+$ cells, which were approximately one-thirds of healthy controls (Tables 2 and 3).

Percentages of total T cells ($CD3^+$), helper T cells ($CD4^+$), cytotoxic T cells ($CD8^+$), B cells ($CD19^+$), and NK cells ($CD56^+$) were comparable to those of normal subjects (Table 4). Interestingly, the majority of $CD4^+$ and $CD8^+$ T cells in Patient 1 were CD45RO-positive, suggesting marked T cell activation. Reflecting this activated status of T cells, Patient 1 showed higher percentages of $HLA\text{-}DR^+CD3^+$ T cells than normal individuals. Such T cell activation defined by CD45RO expression was not observed in the other three patients. As shown in Table 1, Patient 1 has a frame shift mutation and

Table 2 Frequencies of $FOXP3^+CD25^+$ T cells at various ages

Subjects	No.	%$FOXP3^+CD25^+$ cells in $CD4^+$ T cells	%Total $CD25^+$ cells in $CD4^+$ T cells	% $FOXP3^+$ cells in $CD4^+$ $CD25^+$ T cells
Cord blood	12	2.87±1.45 (1.45 4.95)**	10.2±3.7 (3.7 15.2)*	30.0±13.1 (13.1 44.3)
4 14 days	14	4.66±1.85 (1.64 8.45)	12.7±2.4 (9.3 16.4)***	36.7±14.0 (17.0 59.3)
1 2 months	13	3.95±0.97 (2.82 5.74)	11.8±2.3 (9.1 15.2)**	33.8±7.1 (20.1 48.5)
4 9 months	9	4.18±1.17 (2.41 5.98)	12.2±3.5 (7.2 17.6)****	34.9±6.1 (28.3 44.3)
1 3 years	27	4.54±1.71 (2.24 7.86)	13.2±3.4 (8.0 20.2)***	34.8±11.3 (19.1 60.8)
4 6 years	12	5.33±1.68 (3.39 8.60)	14.5±2.4 (10.9 19.9)	35.4±8.5 (24.5 50.9)
7 12 years	25	4.48±1.19 (2.77 6.38)	14.8±3.3 (9.5 19.1)	30.3±4.6 (0.22 39.2)
13 18 years	14	4.57±1.27 (2.13 6.93)	15.5±2.8 (8.6 19.2)	29.7±7.4 (16.7 47.3)
Adult	21	4.57±1.12 (3.09 7.16)	15.7±3.2 (9.2 19.2)	30.1±7.7 (18.0 46.4)

Values are mean±SD. Parentheses indicate the ranges of respective values.
*$P<0.0003$, **$P<0.001$, ***$P<0.02$, ****$P<0.03$ as compared with adult subjects.

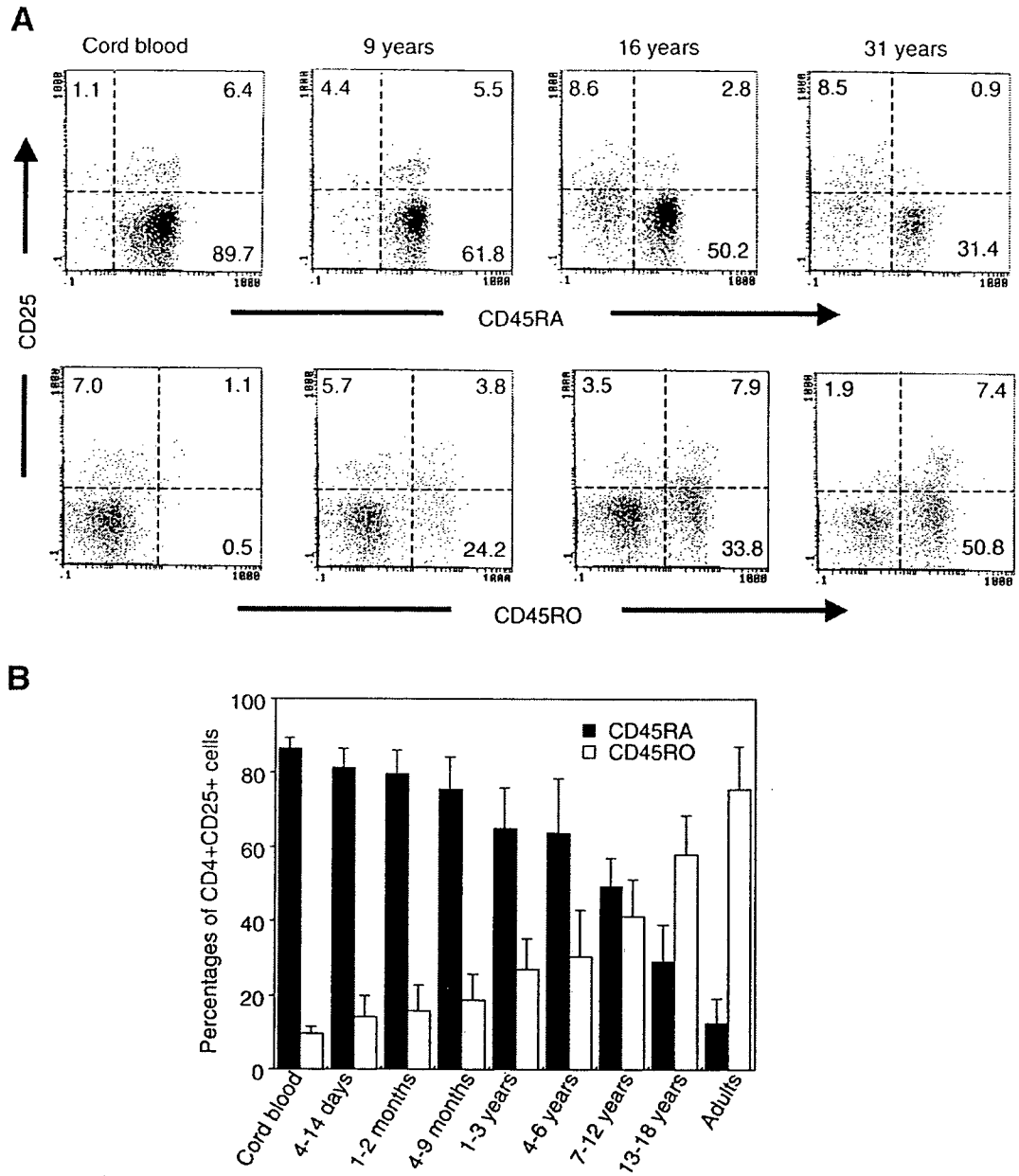

Figure 2 Expression of CD25 and CD45 isoforms by circulating $CD4^+$ T cells of different age groups. Freshly isolated MNC were simultaneously stained for CD25, CD45 RA or CD45RO, and CD4. The relation between CD25 and CD45 isoforms expressed in $CD4^+$ T cell population was analyzed by flow cytometry. (A) Representative staining is shown for different age groups. The numbers in each quadrant indicate percentages of the respective subpopulation. (B) The frequencies of $CD45RA^+$ cells (closed bars) or $CD45RO^+$ cells (open bars) in $CD4^+CD25^+$ T cell population were calculated. Results are expressed as mean values ± SD.

presented with the most severe phenotypes and multiple autoimmune disorders, whereas the other patients have missense mutations and are clinically milder.

Discussion

Treg cells stably expressing FOXP3 are generated in the thymus and released into the circulation as lineage specific $CD4^+CD25^+FOXP3^+$ T cells. Human $CD4^+CD25^-$ T cells if activated *in vitro* have been shown to express FOXP3 and acquire T regulatory activity [14]. However, activation-induced FOXP3 expression is transient and the cells fail to develop suppressor function, suggesting that a sustained high level of FOXP3 expression is required for Treg phenotype and function [25]. Activation of $CD4^+CD25^-$ effector cells in the presence of TGF-β induces the expression of stably high levels of FOXP3 and seems to convert these cells into functional Treg cells [26]. Thus, FOXP3 has emerged as a master control molecule for the generation and function of Treg cells [7,27], which are required not only during fetal

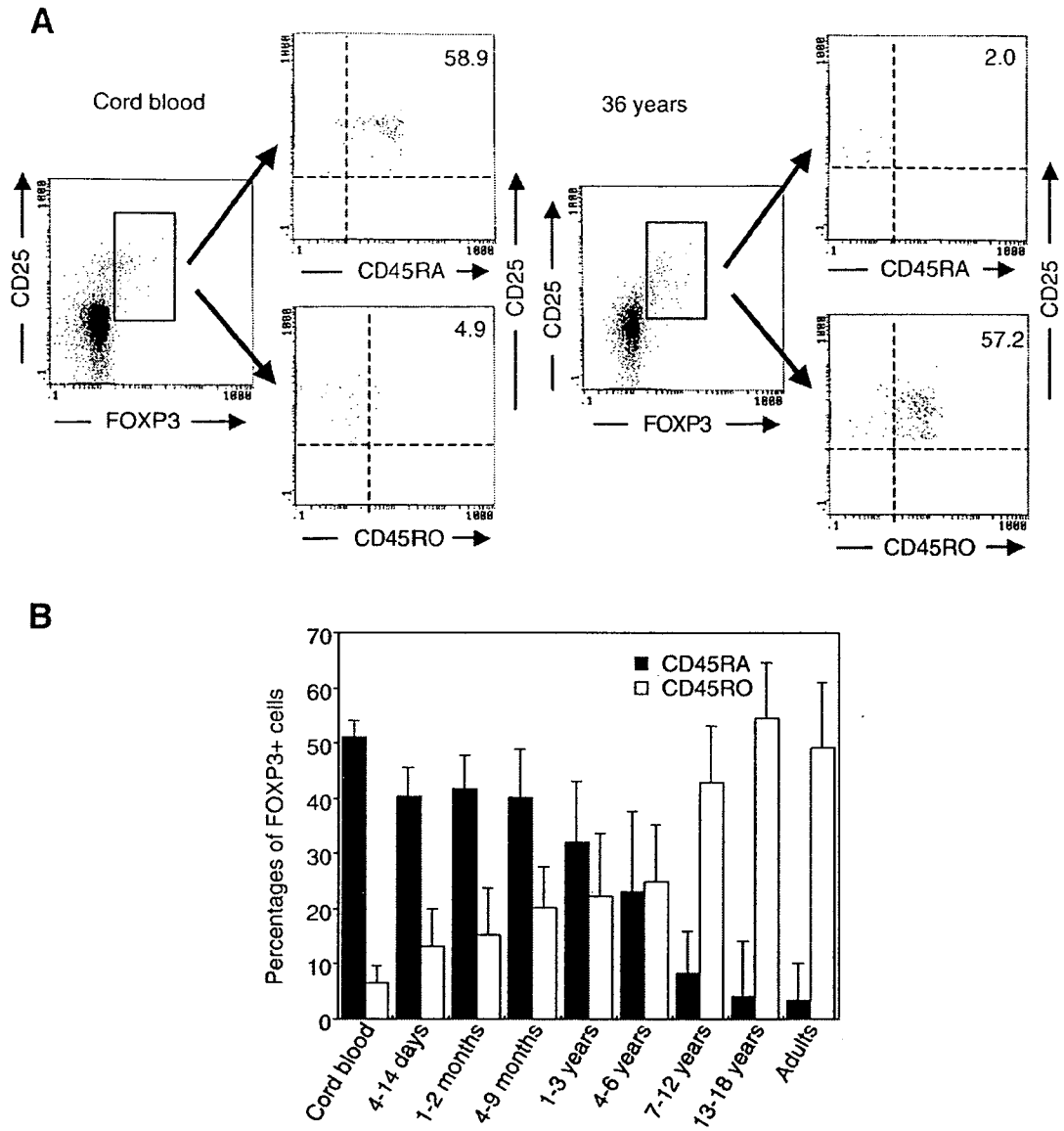

Figure 3 Expression profiles of CD45 isoforms by $CD4^+CD25^+FOXP3^+$ T cells. MNC were simultaneously stained for CD4, CD25, FOXP3, and CD45 RA or CD45RO, and expression profiles of CD45 isoforms in $CD4^+CD25^+FOXP3^+$ T cells were analyzed by flow cytometry. (A) Representative staining of cells obtained from a newborn or an adult subject (on gated $CD4^+$ cells) is shown. The numbers in the upper right quadrant indicate the percentages of the respective subpopulation. (B) The frequency of $CD45RA^+$ cells (closed bars) or $CD45RO^+$ cells (open bars) in the $CD4^+CD25^+FOXP3^+$ T cell population was calculated. Results are expressed as mean values ± SD.

development but throughout the life of mice [28] and possibly humans. Because FOXP3 is the preferred surrogate marker for quantifying human Treg cells [27], monoclonal antibodies designed to recognize FOXP3 protein provide a unique opportunity to study Treg cells at the single cell level [24,25]. Cord blood from fetuses of various gestational ages contains $CD4^+CD25^+$ T cells that express FOXP3 mRNA [19]. However, quantitative data of FOXP3 expressing $CD4^+CD25^+$ Treg cells in cord blood of full-term newborns and in the peripheral blood of children at different ages are not available. In this study, we used a highly specific anti-FOXP3 mAb [24], which is commercially available to determine the proportion of $CD4^+CD25^+FOXP3^+$ cells in the $CD4^+$ lymphocyte population in cord blood and in peripheral blood of infants and children. FOXP3-expressing cells were exclusively found in the $CD4^+CD25^+$ T cell population. The frequency of FOXP3-expressing cells in the $CD4^+$ T cell population was significantly decreased in cord blood of full term newborns and reached adult proportions within the first 2 weeks of life. The percentage of $FOXP3^+$ cells within $CD4^+$ subset remained constant during childhood. $CD4^+CD25^+$ T cells have been identified in lymphoid organs of human fetuses, including thymus, spleen, and lymph nodes, as early as 14 weeks of gestation [29] and were demonstrated in cord blood at 23 weeks gestation [19]. $CD4^+CD25^+$ T cells obtained from cord blood [30] and from fetal thymus or lymph nodes [29,30] expressed FOXP3 at the mRNA level.

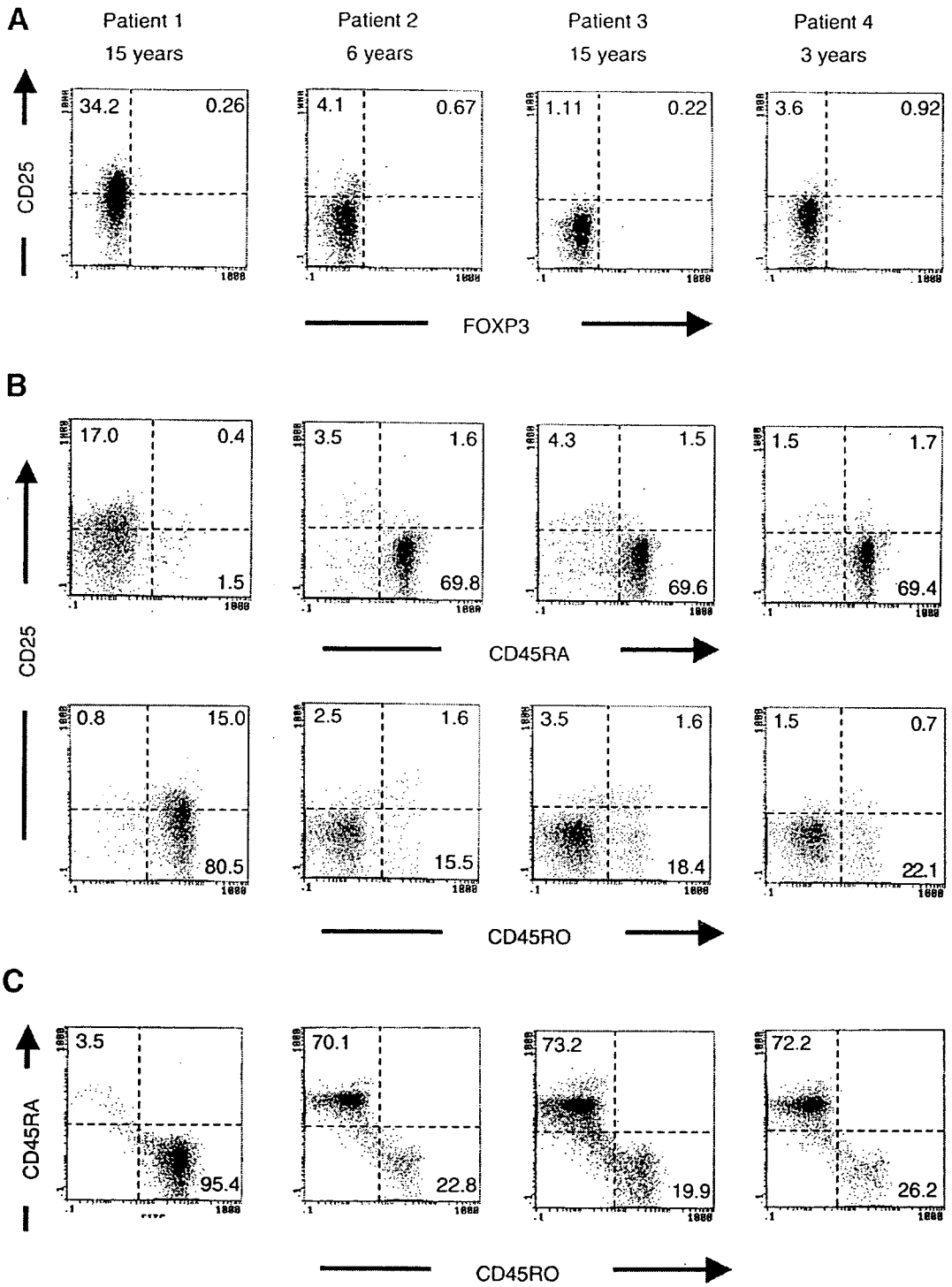

Figure 4 Expression of FOXP3, CD25, and CD45 isoforms in four patients with *FOXP3* gene mutations. (A) Profiles of FOXP3 and CD25 expression, (B) CD25 and CD45 isoform expression, and (C) CD45 isoforms expressed in the circulating CD4⁺ T cell population of each patient. MNC of the patients were stained using a 3-color system and specific mAbs. The numbers in each quadrant indicate percentages of each subpopulation.

By staining single lymphoid cells for FOXP3 expression, we found that CD4⁺CD25⁺ T cells from cord blood predominantly exhibit the naive CD45RA⁺45RO⁻ phenotype which is in agreement with previous reports demonstrating that CD4⁺CD25⁺ T cells isolated from cord blood have a naive phenotype [19,31,32]. As shown in Fig. 2, during infancy and

Table 3 FOXP3-positive $CD4^+CD25^+$ T cells in patients with IPEX

Patient	%$FOXP3^+CD25^+$ cells in $CD4^+$ T cells	%Total $CD25^+$ cells in $CD4^+$ T cells	% $FOXP3^+$ cells in $CD4^+CD25^+$ T cells
Patient 1	0.26	34.5	7.5
Patient 2	0.67	4.7	14.3
Patient 3	0.22	1.4	15.7
Patient 4	0.92	4.5	20.4

Values are mean. Normal controls, see Table 2.

throughout childhood, the proportion of naive Treg cells decreases whereas that of memory Treg cells increases. By the time of puberty (age 13 to 18 years), the $CD4^+45RO^+CD25^+$ $FOXP3^+$ memory Treg population predominates and reaches 50 60% of $FOXP3^+$ Treg cells, confirming earlier observations [16,18]. The standard assay to measure Treg cell function is their ability to suppress proliferation of effector T cells [19,30]. While the results of some studies suggest that both naive and memory Treg cells isolated form adult peripheral blood are strongly suppressive in co-culture experiments [19], others report that only memory Treg cells are immunosuppressive [16]. naive Treg cells exhibit low levels of CD95 and therefore are highly resistant to CD95L-medicated apoptosis, whereas memory Treg cells express high levels of CD95 and are prone to CD95L-mediated apoptosis [33]. These observations suggest that naive Treg cells which are predominantly observed in the peripheral blood of infants and young children are less vulnerable to apoptosis and more likely to survive than memory Treg cells predominating in the adult population. Interestingly, after exposure to anti-CD3/CD28 mAb, cord blood Treg cells strongly upregulate CD95 and become susceptible to CD95L-induced apoptosis [33].

Treg cells are generated as a unique lymphocyte lineage in the thymus and enter the circulation as naive thymus derived Treg cells. If exposed to specific antigens they convert into memory Treg cells, the predominant population in adults. Another source for memory Treg cells is the generation of $CD4^+CD25^+FOXP3^+$ Treg cells from $CD4^+CD25^-$ T cells following TCR stimulation in the secondary lymphoid organs [14,15]. This mechanism may be of importance in view of the finding that memory Treg cells are susceptible to apoptosis. Vukmanovic-Stejic recently demonstrated that $CD4^+CD45RO^+CD25^+FOXP3^+$ Treg cells are highly proliferative *in vivo* with a doubling time of 8 days [18]. These findings suggest that in addition to the thymus derived Treg lineage a large proportion of Treg cells are generated from rapidly dividing, highly differentiated memory $CD4^+$ T cells. Our observation that infants and young children have a predominance of naive Treg cells may be of biologic significance if there are differences in the suppressive effects of naive and memory Treg cells; for instance the two subsets of Treg cells may affect differently the generation of Th2 cells [34] and immunoglobulin production of B cells by affecting differently immunoglobulin class switch recombination [35].

Since FOXP3 is of crucial importance for the development of Treg cells, we examined FOXP3 expressing cells in four IPEX patients from three unrelated families with known FOXP3 mutations. All had very few (<1%) $CD4^+CD45RO^+CD25^+FOXP3^+$ T cells in the peripheral blood when compared with normal controls and the $CD4^+CD25^+$ T cells that were present, were not $CD25^{bright}$. Since it is difficult to clearly distinguish $CD25^{bright}$ from $CD25^{dim}$ cells, it is essential to use FOXP3 expression for the screening of patients suspected to have IPEX.

The patient with most severe IPEX phenotype (patient 1) has a single nucleotide deletion resulting in frame shift and early termination of transcription. The percentage of $CD4^+$ T cells that expressed $CD25^+$ was 35% in patient 1 (but normal in the other 3 IPEX patients with less severe disease and only missense mutations) compared with 16.7% in normal adult individuals. Most of his circulating $CD4^+$ and $CD8^+$ T cells had strongly upregulated activation markers, including CD45RO and HLA-DR, indicating *in vivo* activation. A similar increase in the proportion of $CD25^+$ T cells was observed in an IPEX patient who developed active disease early in life [36]. The murine equivalent of IPEX, the scurfy mouse, develops a rapidly fatal lymphoproliferative disease directly caused by a frame shift mutation in the *FOXP3* gene. Similar to patient 1, scurfy mice present 5- to 8-fold increase in $CD25^+$ T cells compared with normal control mice [37].

Taken together, our study demonstrated a decreased number of Treg cells in cord blood which reaches normal numbers within the first month of life. Measuring single cell expression of FOXP3 we could show an age-dependent progression from predominantly naive ($CD45RA^+$) Treg cells in cord blood to predominantly memory ($CD45RO^+$) Treg cells in late adolescence. The functional implications for these differences between pediatric and adult individuals are presently unknown, but may be important for a better understanding and treatment of the relatively immune

Table 4 Peripheral blood lymphocyte subsets in patients with IPEX

Cell type	Marker	Patient 1	Patient 2	Patient 3	Patient 4	Normal (n=15)
Total T cells	CD3	56.9%	52.4%	52.7%	53.3%	69.5±4.6%
Activated T cells	HLA-DR/CD3	17.25%	2.4%	4.4%	1.8%	<3%
Helper T cells	CD4	39.2%	39.1%	34.3%	35.3%	43.1±6.0%
Memory/activated cells in helper T cells	CD45RO /CD4	95.4%	22.8%	25.2%	26.2%	28.7±9.2%
Cytotoxic T cells	CD8	17.5%	12.4%	19.4%	20.3%	22.0±5.4%
Memory/activated cells in cytotoxic T cells	CD45RO/CD8	85.7%	10.0%	14.5%	7.0%	19.0±1.1%
B cells	CD19	10.1%	31.6%	17.0%	8.4%	11.2±3.5%
Natural killer cells	CD56	12.6%	12.4%	15.4%	3.5%	8.0±4.4%

Values are mean±SD.

incompetence of infants and children compared with adults and may have implications for the treatment of autoimmune disorders, allergic diseases, tumor development, and post transplantation graft vs. host disease. Flow cytometry using an anti-FOXP3 mAb provides a convenient tool to identify IPEX patients by their inability to generate FOXP3 positive Treg cells.

Acknowledgments

We thank Masatoshi Okada (Okada Obstetrics and Gynecology Hospital) for kindly collecting cord blood samples, and Chikako Sakai and Hitoshi Moriuchi for excellent technical assistance. This work was supported by Grant-in-Aid for Scientific Research from the Ministry of Education, Culture, Sports, Science and Technology of Japan, and a grant from Ministry of Health, Labour and Welfare of Japan.

References

[1] S. Sakaguchi, Regulatory T cells: key controllers of immunologic self-tolerance, Cell 101 (2000) 455 458.

[2] Y. Belkaid, C.A. Piccirillo, S. Mendez, E.M. Shevach, D.L. Sacks, CD4+CD25+ regulatory T cells control Leishmania major persistence and immunity, Nature 420 (2002) 502 507.

[3] S. Sakaguchi, Naturally arising Foxp3-expressing CD25+CD4+ regulatory T cells in immunological tolerance to self and non-self, Nat. Immunol. 6 (2005) 345 352.

[4] H. Waldmann, T.C. Chen, L. Graca, E. Adams, S. Daley, S. Cobbold, P.J. Fairchild, Regulatory T cells in transplantation, Semin. Immunol. 18 (2006) 111 119.

[5] M. Akdis, K. Blaser, C.A. Akdis, T regulatory cells in allergy: novel concepts in the pathogenesis, prevention, and treatment of allergic diseases, J. Allergy Clin. Immunol. 116 (2005) 961 968 (quiz 969).

[6] S. Hori, T. Nomura, S. Sakaguchi, Control of regulatory T cell development by the transcription factor Foxp3, Science 299 (2003) 1057 1061.

[7] J.D. Fontenot, M.A. Gavin, A.Y. Rudensky, Foxp3 programs the development and function of CD4+CD25+ regulatory T cells, Nat. Immunol. 4 (2003) 330 336.

[8] T.A. Chatila, F. Blaeser, N. Ho, H.M. Lederman, C. Voulgaropoulos, C. Helms, A.M. Bowcock, JM2, encoding a fork head-related protein, is mutated in X-linked autoimmunity-allergic disregulation syndrome, J. Clin. Invest. 106 (2000) R75 R81.

[9] M.E. Brunkow, E.W. Jeffery, K.A. Hjerrild, B. Paeper, L.B. Clark, S.A. Yasayko, J.E. Wilkinson, D. Galas, S.F. Ziegler, F. Ramsdell, Disruption of a new forkhead/winged-helix protein, scurfin, results in the fatal lymphoproliferative disorder of the scurfy mouse, Nat. Genet. 27 (2001) 68 73.

[10] R.S. Wildin, F. Ramsdell, J. Peake, F. Faravelli, J.L. Casanova, N. Buist, E. Levy-Lahad, M. Mazzella, O. Goulet, L. Perroni, F.D. Bricarelli, G. Byrne, M. McEuen, S. Proll, M. Appleby, M.E. Brunkow, X-linked neonatal diabetes mellitus, enteropathy and endocrinopathy syndrome is the human equivalent of mouse scurfy, Nat. Genet. 27 (2001) 18 20.

[11] C.L. Bennett, J. Christie, F. Ramsdell, M.E. Brunkow, P.J. Ferguson, L. Whitesell, T.E. Kelly, F.T. Saulsbury, P.F. Chance, H.D. Ochs, The immune dysregulation, polyendocrinopathy, enteropathy, X-linked syndrome (IPEX) is caused by mutations of FOXP3, Nat. Genet. 27 (2001) 20 21.

[12] P.J. Blair, S.J. Bultman, J.C. Haas, B.T. Rouse, J.E. Wilkinson, V.L. Godfrey, CD4+CD8- T cells are the effector cells in disease pathogenesis in the scurfy (sf) mouse, J. Immunol. 153 (1994) 3764 3774.

[13] H.D. Ochs, S.F. Ziegler, T.R. Torgerson, FOXP3 acts as a rheostat of the immune response, Immunol. Rev. 203 (2005) 156 164.

[14] M.R. Walker, D.J. Kasprowicz, V.H. Gersuk, A. Benard, M. Van Leghen, J.H. Buckner, S.F. Ziegler, Induction of FoxP3 and acquisition of T regulatory activity by stimulated human CD4+CD25- T cells, J. Clin. Invest. 112 (2003) 1437 1443.

[15] Z. Wang, J. Hong, W. Sun, G. Xu, N. Li, X. Chen, A. Liu, L. Xu, B. Sun, J.Z. Zhang, Role of IFN-gamma in induction of Foxp3 and conversion of CD4+ CD25- T cells to CD4+ Tregs, J. Clin. Invest. 116 (2006) 2434 2441.

[16] H. Yagi, T. Nomura, K. Nakamura, S. Yamazaki, T. Kitawaki, S. Hori, M. Maeda, M. Onodera, T. Uchiyama, S. Fujii, S. Sakaguchi, Crucial role of FOXP3 in the development and function of human CD25+CD4+ regulatory T cells, Int. Immunol. 16 (2004) 1643 1656.

[17] C. Baecher-Allan, J.A. Brown, G.J. Freeman, D.A. Hafler, CD4+CD25high regulatory cells in human peripheral blood, J. Immunol. 167 (2001) 1245 1253.

[18] M. Vukmanovic-Stejic, Y. Zhang, J.E. Cook, J.M. Fletcher, A. McQuaid, J.E. Masters, M.H. Rustin, L.S. Taams, P.C. Beverley, D.C. Macallan, A.N. Akbar, Human CD4+ CD25hi Foxp3+ regulatory T cells are derived by rapid turnover of memory populations in vivo, J. Clin. Invest. 116 (2006) 2423 2433.

[19] Y. Takahata, A. Nomura, H. Takada, S. Ohga, K. Furuno, S. Hikino, H. Nakayama, S. Sakaguchi, T. Hara, CD25+CD4+ T cells in human cord blood: an immunoregulatory subset with naive phenotype and specific expression of forkhead box p3 (Foxp3) gene, Exp. Hematol. 32 (2004) 622 629.

[20] D. Valmori, A. Merlo, N.E. Souleimanian, C.S. Hesdorffer, M. Ayyoub, A peripheral circulating compartment of natural naive CD4 Tregs, J. Clin. Invest. 115 (2005) 1953 1962.

[21] N. Seddiki, B. Santner-Nanan, S.G. Tangye, S.I. Alexander, M. Solomon, S. Lee, R. Nanan, B.F. de Saint Groth, Persistence of naive CD45RA+ regulatory T cells in adult life, Blood 107 (2006) 2830 2838.

[22] I. Kobayashi, R. Shiari, M. Yamada, N. Kawamura, M. Okano, A. Yara, A. Iguchi, N. Ishikawa, T. Ariga, Y. Sakiyama, H.D. Ochs, K. Kobayashi, Novel mutations of FOXP3 in two Japanese patients with immune dysregulation, polyendocrinopathy, enteropathy, X linked syndrome (IPEX), J. Med. Genet. 38 (2001) 874 876.

[23] H. Tanaka, K. Suzuki, T. Nakahata, I. Kobayashi, M. Kubota, E. Ito, Immune dysregulation, polyendocrinopathy, enteropathy, X-linked syndrome, Acta Paediatr. 93 (2004) 142 143.

[24] G. Roncador, P.J. Brown, L. Maestre, S. Hue, J.L. Martinez-Torrecuadrada, K.L. Ling, S. Pratap, C. Toms, B.C. Fox, V. Cerundolo, F. Powrie, A.H. Banham, Analysis of FOXP3 protein expression in human CD4+CD25+ regulatory T cells at the single-cell level, Eur. J. Immunol. 35 (2005) 1681 1691.

[25] M.A. Gavin, T.R. Torgerson, E. Houston, P. DeRoos, W.Y. Ho, A. Stray-Pedersen, E.L. Ocheltree, P.D. Greenberg, H.D. Ochs, A.Y. Rudensky, Single-cell analysis of normal and FOXP3-mutant human T cells: FOXP3 expression without regulatory T cell development, Proc. Natl. Acad. Sci. U. S. A. 103 (2006) 6659 6664.

[26] M.C. Fantini, C. Becker, I. Tubbe, A. Nikolaev, H.A. Lehr, P. Galle, M.F. Neurath, Transforming growth factor beta induced FoxP3+ regulatory T cells suppress Th1 mediated experimental colitis, Gut 55 (2006) 671 680.

[27] A.H. Banham, F.M. Powrie, E. Suri-Payer, FOXP3+ regulatory T cells: current controversies and future perspectives, Eur. J. Immunol. 36 (2006) 2832 2836.

[28] J.M. Kim, J.P. Rasmussen, A.Y. Rudensky, Regulatory T cells prevent catastrophic autoimmunity throughout the lifespan of mice, Nat. Immunol. 8 (2007) 191 197.

[29] T. Cupedo, M. Nagasawa, K. Weijer, B. Blom, H. Spits, Development and activation of regulatory T cells in the human fetus, Eur. J. Immunol. 35 (2005) 383 390.

[30] K. Wing, P. Larsson, K. Sandstrom, S.B. Lundin, E. Suri-Payer, A.